

RESEARCH ARTICLE

10.1002/2013JG002520

Key Points:

- Two year average CH₄ flux from a marsh was compatible with its net CO₂ uptake
- CH₄ flux was regulated by different factors at diurnal and seasonal scales
- Plant-modulated gas flow and inundation led to high CH₄ flux from the marsh

Supporting Information:

- Readme
- Figure S1
- Figure S2
- Table S1
- Table S2
- Table S3
- Table S4
- Table S5
- Table S6
- Table S7
- Text S1

Correspondence to:

H. Chu,
hchu6@rockets.utoledo.edu

Citation:

Chu, H., J. Chen, J. F. Gottgens, Z. Ouyang, R. John, K. Czajkowski, and R. Becker (2014), Net ecosystem methane and carbon dioxide exchanges in a Lake Erie coastal marsh and a nearby cropland, *J. Geophys. Res. Biogeosci.*, 119, doi:10.1002/2013JG002520.

Received 27 SEP 2013

Accepted 28 MAR 2014

Accepted article online 7 APR 2014

Net ecosystem methane and carbon dioxide exchanges in a Lake Erie coastal marsh and a nearby cropland

Housen Chu¹, Jiquan Chen¹, Johan F. Gottgens¹, Zutao Ouyang¹, Ranjeet John¹, Kevin Czajkowski², and Richard Becker¹

¹Department of Environmental Sciences, University of Toledo, Toledo, Ohio, USA, ²Department of Geography and Planning, University of Toledo, Toledo, Ohio, USA

Abstract Net ecosystem carbon dioxide (F_{CO₂}) and methane (F_{CH₄}) exchanges were measured by using the eddy covariance method to quantify the atmospheric carbon budget at a *Typha*- and *Nymphaea*-dominated freshwater marsh (March 2011 to March 2013) and a soybean cropland (May 2011 to May 2012) in northwestern Ohio, USA. Two year average annual F_{CH₄} (49.7 g C-CH₄ m⁻² yr⁻¹) from the marsh was high and compatible with its net annual CO₂ uptake (F_{CO₂}: -21.0 g C-CO₂ m⁻² yr⁻¹). In contrast, F_{CH₄} was small (2.3 g C-CH₄ m⁻² yr⁻¹) and accounted for a minor portion of the atmospheric carbon budget (F_{CO₂}: -151.8 g C-CO₂ m⁻² yr⁻¹) at the cropland. At the seasonal scale, soil temperature associated with methane (CH₄) production provided the dominant regulator of F_{CH₄} at the marsh (R² = 0.86). At the diurnal scale, plant-modulated gas flow was the major pathway for CH₄ outgassing in the growing season at the marsh. Diffusion and ebullition became the major pathways in the nongrowing season and were regulated by friction velocity. Our findings highlight the importance of freshwater marshes for their efficiency in turning over and releasing newly fixed carbon as CH₄. Despite marshes accounting for only ~4% of area in the agriculture-dominated landscape, their high F_{CH₄} should be carefully addressed in the regional carbon budget.

1. Introduction

Wetlands, the largest natural sources of methane (CH₄), were shown to have profound effects in driving the atmospheric CH₄ concentration in recent decades [Bridgman *et al.*, 2006]. It has been documented that climatic variations have resulted in large interannual variations of CH₄ emissions from wetlands since the 1980s [Bousquet *et al.*, 2006; Bridgman *et al.*, 2012]. Considering both the direct and indirect contributions of CH₄ to radiative forcing, the warming effect of releasing 1 g CH₄ into the atmosphere is 25 times that of releasing an equivalent mass of carbon dioxide (CO₂) on a 100 year time horizon [Forster *et al.*, 2007]. The interplay of the net ecosystem CO₂ (F_{CO₂}) and CH₄ (F_{CH₄}) exchanges in terms of the wetland greenhouse gas budget and global warming effects is still under debate [e.g., Hendriks *et al.*, 2007; Mitsch and Gosselink, 2007; Mitsch *et al.*, 2012; Song *et al.*, 2009]. While inundation of wetlands reduces the aerobic decomposition (i.e., CO₂ production) and enhances the sediment deposition rate, such inundation also enhances the anaerobic decomposition and thus CH₄ generation [Mitsch and Gosselink, 2007]. Recent studies suggest that greenhouse effects, mitigated by the uptake of CO₂ by wetland vegetation, could be partly or entirely offset by CH₄ emission [e.g., Frohling *et al.*, 2006; Hendriks *et al.*, 2007; Olson *et al.*, 2013; Song *et al.*, 2009]. Frohling *et al.* [2006] documented that the net warming effects of CH₄ may persist for hundreds to thousands of years before being compensated by the CO₂ uptake of wetlands. Hence, a better comprehension of the wetland greenhouse gas budget and its regulation is urgently needed in order to better understand the resilience of wetland ecosystems and formulate adaptive management plans under global climate change.

Recent advances in theory and instrumentation have facilitated the extensive application of tower-based eddy covariance measurements [Baldochi *et al.*, 2001; Dabberdt *et al.*, 1993]. These advances benefit the spatially integrative measurement of ecosystem-scale mass and energy fluxes [Baldochi *et al.*, 1988], greatly enhancing our understanding of the biogeochemical processes driving these fluxes [e.g., Jung *et al.*, 2010; Tan *et al.*, 2012; Yi *et al.*, 2010]. The quasi-continuous measurement of these fluxes and ancillary physical variables (e.g., incident radiation, temperature) also allows researchers to examine these fluxes and construct suitable models from a half-hourly to a decadal scale [e.g., Richardson *et al.*, 2007; Teklemariam *et al.*, 2010; Wu *et al.*,

2012]. In addition, progress in integrating the eddy covariance measurements with satellite-based vegetation indices (e.g., normalized difference vegetation index, NDVI) provides researchers with a more comprehensive approach for examining the interaction between mass/energy fluxes and vegetation characteristics [Lieth, 1974; Xiao *et al.*, 2009].

While many sizeable efforts have been devoted to F_{CO_2} research, less research has attempted to quantify F_{CH_4} using the eddy covariance method (see earlier works in Edwards *et al.* [1994], Hargreaves and Fowler [1998], and Verma *et al.* [1992]). Only recently have a few papers examined the annual and interannual variability of F_{CH_4} in addition to F_{CO_2} [Hatala *et al.*, 2012; Herbst *et al.*, 2011a; Kroon *et al.*, 2010; Olson *et al.*, 2013]. These pioneer studies suggested that CH_4 contributes a significant portion to the wetland greenhouse gas budget. In addition, the wetland F_{CH_4} is sensitive to the interannual variations of hydrometeorological conditions [Olson *et al.*, 2013; Tagesson *et al.*, 2012] and land management [Hatala *et al.*, 2012; Herbst *et al.*, 2013]. Hence, a wide range of F_{CH_4} (10^{-1} – 10^2 g C- CH_4 m $^{-2}$ yr $^{-1}$) has been reported among sites and years.

In this study, we targeted a temperate freshwater marsh and a conventional cropland in northwestern Ohio, USA, in an area that was once occupied by the Great Black Swamp (~ 4000 km 2) [Mitsch and Gosselink, 2007]. The Great Black Swamp was extensively drained starting in the 1850s and was largely converted into cropland during 1850–1890. Currently, croplands and forests account for $\sim 70\%$ and $\sim 7\%$ of the land cover in the region, respectively. Only $\sim 4\%$ of wetlands (~ 150 km 2 , mostly marshes) remain in the region and most of them are managed for waterfowl conservation [Mitsch and Gosselink, 2007]. For this purpose of waterfowl conservation, water levels in these wetlands are often managed, including inputs from nearby agricultural drainages. Gottgens and Liptak [1998] highlighted that these wetlands receive a considerable amount of nutrients and organic carbon from the nearby croplands through agricultural runoff. It is not clear how the current management may influence the dynamics of F_{CH_4} and F_{CO_2} in these wetlands and to what extent these wetlands may contribute to the regional carbon budget. As these wetlands are located within an agriculture-dominated landscape and connected hydrologically with nearby croplands, we argued that their importance needs to be examined in the context of this landscape. In this study, we aimed to address the following questions: (1) What are the contributions of F_{CH_4} and F_{CO_2} to the atmospheric carbon budget at the freshwater marsh in comparison with the nearby cropland? (2) At the ecosystem and regional scales, will the carbon released via F_{CH_4} be compensated by the carbon uptake via F_{CO_2} ? (3) What are the physical and biological regulators of F_{CH_4} at the marsh and the cropland sites and how do these controls vary from half-hourly to yearly scales?

2. Materials and Methods

2.1. Study Sites

The targeted freshwater marsh is located in the Winous Point Marsh Conservancy along the shore of Lake Erie (N41°27'51.28", W82°59'45.02"; Figure 1). A conventional cropland located in Curtice, Ohio (N41°37'42.31", W83°20'43.18") is included in order to provide a background F_{CH_4} and F_{CO_2} from the agriculture-dominated ($\sim 70\%$) region, where soybean (*Glycine max*) and corn (*Zea mays*) are the major crops. The two sites are ~ 30 km apart and have similar climate conditions with a regional mean temperature of $\sim 9.2^\circ\text{C}$ and annual precipitation of ~ 840 mm in the last 30 years [Noormets *et al.*, 2008].

The marsh site has been owned by the Winous Point Shooting Club since 1856 and has been managed by wildlife biologists since 1946 [Gottgens *et al.*, 1998]. The hydrology of the marsh is relatively isolated by the surrounding dikes and drainages and only receives drainage from nearby croplands through three connecting ditches [Gottgens and Liptak, 1998]. Since 2001, the marsh has been managed to maintain year-round inundation with the lowest water levels in September. A 3 m triangular tower was built at the center of the 129 ha North Marsh in July 2010 (Figure 1). Within the 0–250 m fetch of the tower, the marsh comprises 42.9% of floating-leaved vegetation, 52.7% of emergent vegetation, and 4.4% of dike and upland during the growing season. Floating-leaved vegetation covers the majority of area near the tower and extends about 60–150 m from the tower (Figure 1). Dominant emergent plants include narrow-leaved cattail (*Typha angustifolia*), rose mallow (*Hibiscus moscheutos*), and bur reed (*Sparganium americanum*). Common floating-leaved species are water lily (*Nymphaea odorata*) and American lotus (*Nelumbo lutea*) with foliage usually covering the water surface from late May to early October. *Nymphaea* and *Nelumbo* start to shed leaves after

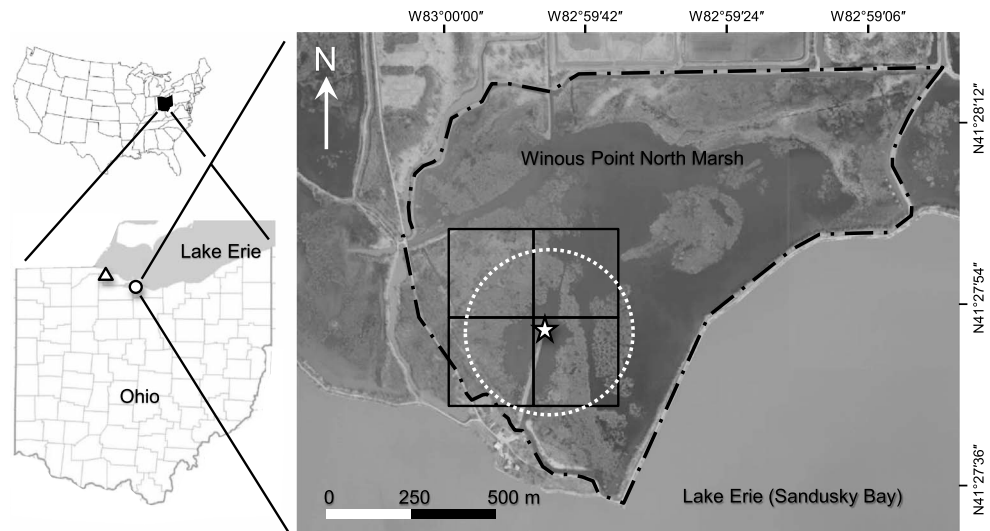


Figure 1. Map of the study marsh (open circle) and cropland (open triangle) in northwestern Ohio, USA. The background aerial photo was obtained through the Ohio Geographically Referenced Information Program in the State of Ohio Office of Information Technology. The target marsh (Winous Point North Marsh) is highlighted by the dash-dotted polygon. The aerial photo was taken on 13 April in 2011 before the floating-leaved plants emerged and covered the open water area (dark grey area). The light grey area in the marsh indicates the emergent vegetation area. The star and dotted circle indicate the tower location and the 250 m fetch. The black square represents the geolocation of the four $250 \times 250 \text{ m}^2$ pixels of the normalized difference vegetation index (NDVI, MOD13Q1) obtained from the Moderate Resolution Imaging Spectroradiometer (MODIS) instrument.

early October and the floating-leaved vegetation area turns to open water through the winter and early spring. The aboveground biomass (\pm SD) is 0.22 ± 0.03 and $1.52 \pm 0.27 \text{ kg C m}^{-2}$ in the floating-leaved and emergent vegetation areas, respectively, while the belowground biomass is 0.21 ± 0.10 and $12.55 \pm 3.87 \text{ kg C m}^{-2}$, respectively. The vegetation biomass was harvested at 14 randomly selected $0.5 \times 0.5 \text{ m}^2$ plots, of which six and eight plots were dominated with floating-leaved and emergent vegetation, respectively. The soil is classified as hydric and the organic layer extends to a depth of 15–30 cm. The soil is clay-rich mineral beneath the organic layer.

A 3 m triangular tower was installed at the center of a 50 ha soybean cropland in July 2010 and had at least 300 m of homogeneous fetch in all directions. The cropland site is rain fed and no irrigation is applied. As it is located in a part of the historic Great Black Swamp, drainage tiles are deployed around 0.5–1.0 m beneath the ground surface in order to draw down the water level. The soil is classified as silty clay and silty clay loam. The cultivation practices include minimum tillage and both insect and weed control. Soybeans were planted and harvested on 10 June and 23 October in 2011, respectively. The aboveground and belowground soybean biomass (\pm SD) were 0.42 ± 0.01 and $0.05 \pm 0.01 \text{ kg C m}^{-2}$ at the peak growing season in 2011, with a leaf area index of 3.6 ± 0.4 .

2.2. Flux Measurements and Calculations

The eddy covariance method was applied to quantify F_{CO_2} and F_{CH_4} at both sites. The system, including a sonic anemometer (CSAT3, Campbell Sci., Inc., Logan, UT, USA (CSI)), an open path $\text{CO}_2/\text{H}_2\text{O}$ infrared gas analyzer (LI7500, LI-COR, Cor., Lincoln, NE, USA (LI-COR)), and an open path CH_4 gas analyzer (LI7700, LI-COR), was mounted 2 m above the water (marsh)/soil (cropland) surface. The height was determined to ensure that the eddy covariance system is mounted at least twice the height of the nearby canopy (0.4–0.6 m and 0.8–1.0 m at the marsh and cropland, respectively) in the peak growing season. The measurement periods were 12 March 2011 to 27 March 2013 (2 years), and 10 May 2011 to 10 May 2012 (1 year) at the marsh and cropland sites, respectively. The raw data were sampled with a 10 Hz frequency and recorded by the CR5000 data logger. Both LI7500 and LI7700 were calibrated routinely in the laboratory (see Table S1 for calibration standards in the supporting information).

F_{CO_2} and F_{CH_4} were calculated following the FLUXNET methodology [Aubinet *et al.*, 2000]. All calculations were performed with EdiRe (University of Edinburgh, v1.5.0.29, 2011) following the workflow described in Chu *et al.* [2013, 2014]. The details of the general flux calculation and uncertainty estimation were discussed in the supporting information (Text S1). In addition, the relative signal strength indicator (RSSI) was adopted to screen out the periods when the mirror of LI7700 was contaminated by rainfall or dust ($\text{RSSI} < 10\%$) [McDermitt *et al.*, 2011]. We set the LI7700 to check the signal strength at 0800 h everyday. A cleaning solution (alcohol/water mixture) was applied to clean the mirror every 10 min between 0800 h and 0900 h until the signal strength recovered. The cleaning protocol was determined to ensure that the LI7700 resumes quality CH_4 measurements no later than 1 day after the intense rainfalls. The LI7700-specific correction was also applied to correct the spectroscopic effects [LI-COR, 2010]. The footprint contribution for each half-hourly flux was examined by using the model developed by Kormann and Meixner [2001]. The majority of footprint ($> 80\%$) was located within the 0–250 m fetch at both sites (details in Text S1 and Table S2). At the marsh site, floating-leaved vegetation covered the majority of the area near the tower and extended 80–150 m from the tower in the prevailing wind direction (225° – 315°). Thus, floating-leaved vegetation area contributed to $\sim 74\%$ of the measured flux at the marsh. In this study, positive F_{CO_2} and F_{CH_4} indicate a net flux from the ecosystem to the atmosphere. A near-neutral atmospheric carbon budget was defined when the reported F_{CO_2} and F_{CH_4} were not significantly different from zero based on the 95% uncertainty intervals.

2.3. Gap Filling and Partitioning of F_{CO_2}

Overall, 63% and 54% of F_{CO_2} passed the quality control checks at the marsh and cropland sites, respectively. Data gaps of F_{CO_2} were filled using the marginal distribution sampling method [Reichstein *et al.*, 2005]. F_{CO_2} was further decomposed into gross ecosystem production (GEP) and ecosystem respiration (ER) following Reichstein *et al.* [2005]. Both GEP and ER were presented with positive signs ($F_{\text{CO}_2} = \text{ER} - \text{GEP}$). The uncertainties of flux partitioning were obtained through uncertainty propagation via the Monte Carlo simulations ($N = 1000$) technique of Richardson and Hollinger [2005]. More details on the modeling and partitioning processes are discussed in the supporting information (Text S1). The start and end of the growing season were identified as the first and last consecutive 3 days with detectable daily GEPs ($> 1 \text{ g C-CO}_2 \text{ m}^{-2} \text{ d}^{-1}$) [Barr *et al.*, 2009].

2.4. Modeling and Gap Filling of F_{CH_4}

Overall, 40% and 42% of F_{CH_4} passed the quality control checks at the marsh and cropland sites, respectively. Our data coverage was compatible with reports from the few available short-term studies (< 1 year) that also used LI7700 to measure F_{CH_4} (45–46%) [Dengel *et al.*, 2011; Yu *et al.*, 2013]. We adopted the marginal distribution sampling method in F_{CH_4} gap filling and modified the method slightly by including friction velocity (u_*) in selecting the similar micrometeorological conditions. The marginal distribution sampling method takes advantage of the autocorrelation and short-term dependency of the flux data. Hence, the marginal distribution sampling method is capable of incorporating the unmeasured factors (e.g., phenology, substrate quality) and filling the flux gaps when a robust regression model is not available (e.g., F_{CH_4} at the cropland in the study).

In addition, the linear regression model was adopted in order to explore the regulation of F_{CH_4} at different temporal scales. First, we examined the daily-to-yearly regulation by exploring the relationship between the daily F_{CH_4} and biophysical factors. We selected soil temperature, u_* , and groundwater level as the targeted physical factors. The biological regulation was examined via exploring the relationship between the daily F_{CH_4} and GEP. The significance test and stepwise model simplification were performed following the method described in Chu *et al.* [2014]. More details on the modeling processes are discussed in the supporting information (Text S1).

Second, we adopted a moving window multiple linear regression in examining the regulation of F_{CH_4} from a half-hourly to weekly scale. We applied a nonoverlapping moving window with a fixed width of 8 days to the entire time series. A separate regression was fitted for each 8 day period. The window size was determined to include a sufficient number of data ($N > 48$) while not to introduce the seasonality of F_{CH_4} . Soil temperature, u_* , and groundwater level were chosen as the predictor variables. After

preliminary data exploration, we log transformed F_{CH_4} and fit it with a multiple linear regression model [Wille *et al.*, 2008]:

$$\ln(F_{CH_4}) = \ln(R_{FCH_4.1}) + S_{Tg} \left(\frac{T_g - \overline{T_g}}{10} \right) + S_{u^*} \left(\frac{u_* - \overline{u_*}}{0.1} \right) + S_{WT} \left(\frac{WT - \overline{WT}}{0.1} \right) \quad (1)$$

where the overbar indicates the mean value in each period, $R_{FCH_4.1}$ ($\text{nmol m}^{-2} \text{s}^{-1}$) is the base F_{CH_4} at the period-averaged soil temperature (T_g ($^{\circ}\text{C}$)), u_* (m s^{-1}), and groundwater level (WT (m)), and S_{Tg} , S_{u^*} , and S_{WT} represent the sensitivities of F_{CH_4} to every 10°C change in soil temperature, every 0.1 m s^{-1} change in u_* , and every 0.1 m change in groundwater level, respectively. For the marsh site, we further examined the plant modulation via the relationship of F_{CH_4} against air temperature and vapor pressure deficit (VPD) in the growing season. Air temperature and VPD were used here because they were documented as the main drivers of plant-modulated gas flow [Brix *et al.*, 1992; Dacey, 1981; Grosse, 1996; Tornberg *et al.*, 1994]:

$$\ln(F_{CH_4}) = \ln(R_{FCH_4.2}) + S_{Ta} \left(\frac{T_a - \overline{T_a}}{10} \right) + S_{VPD} \left(\frac{VPD - \overline{VPD}}{0.1} \right) \quad (2)$$

where $R_{FCH_4.2}$ ($\text{nmol m}^{-2} \text{s}^{-1}$) is the base F_{CH_4} at the period-averaged air temperature (T_a ($^{\circ}\text{C}$)) and VPD (kPa), and S_{Ta} and S_{VPD} represent the sensitivities of F_{CH_4} to every 10°C change in air temperature and every 0.1 kPa change in VPD, respectively. More details of the modeling processes are discussed in the supporting information (Text S1).

2.5. Micrometeorology Measurements

Micrometeorological variables were measured at both tower sites (details of the sensor types and mounting locations are listed in Table S1), including long-/short-wave radiation, albedo, photosynthetically active radiation (PAR), air temperature, relative humidity, VPD, precipitation, soil temperature (at 0.1 and 0.3 m depth), groundwater level, volumetric soil water content (only at the cropland), and surface water temperature (only at the marsh). Because surface water temperature was measured at fixed locations (0.1 and 0.3 m) above the sediment, recorded surface water temperature may not have reached 0°C when only the uppermost layer of surface water was frozen in the winter. We adopted albedo as an indicator in distinguishing the periods with frozen ice/snow cover (albedo > 0.2) from those with open water (albedo < 0.2) [Bonan, 2002]. All of the variables were sampled every second and recorded every 30 min by the data logger (CR5000, CSI).

Regional long-term meteorological data (i.e., air temperature and precipitation) were obtained through the National Climatic Data Center of the National Oceanic and Atmospheric Administration, USA. Three weather stations, Bowling Green (N41 $^{\circ}$ 22'59", W83 $^{\circ}$ 36'39", 1893–2013), Fremont (N41 $^{\circ}$ 19'59", W83 $^{\circ}$ 07'08", 1901–2013), and Toledo Express Airport (N41 $^{\circ}$ 35'18", W83 $^{\circ}$ 48'05", 1955–2013), were selected because they all had more than 50 years of records and are located less than 30 km from our sites.

2.6. Satellite-Based Vegetation Index

We adopted NDVI as the land surface vegetation index in order to provide seasonal vegetation dynamics [Morissette *et al.*, 2008; Zhang *et al.*, 2003]. NDVI has been documented to adequately quantify the ecosystem-level vegetation dynamics (e.g., canopy coverage, greenness, and biomass) in wetlands and croplands [Jialin, 2011; Lunetta *et al.*, 2010]. The 16 day NDVI data (MOD13Q1) of the Moderate Resolution Imaging Spectroradiometer (MODIS) instrument were obtained from the Land Process Distributed Active Archive Center, US Geological Survey, USA. The target spatial coverage was the nearest four $250 \times 250 \text{ m}^2$ MODIS pixels around the marsh and cropland flux towers (Figure 1). The spatial extent was determined in correspondence with the major footprint of the flux measurement. The long-term NDVI trend was calculated from 2000 to 2012. Additionally, we conducted a series of in situ surface reflectance measurements in order to examine the suitability of MODIS NDVI in such a confined spatial extent ($500 \times 500 \text{ m}^2$). In general, our upscale $500 \times 500 \text{ m}^2$ NDVI from the ground spectrometer measurements showed agreements with the MODIS NDVI, suggesting that the MODIS NDVI adequately monitored the ecosystem-scale vegetation dynamics at both sites. The details of the in situ surface reflectance measurements and the validation processes are discussed in the supporting information (Text S1).

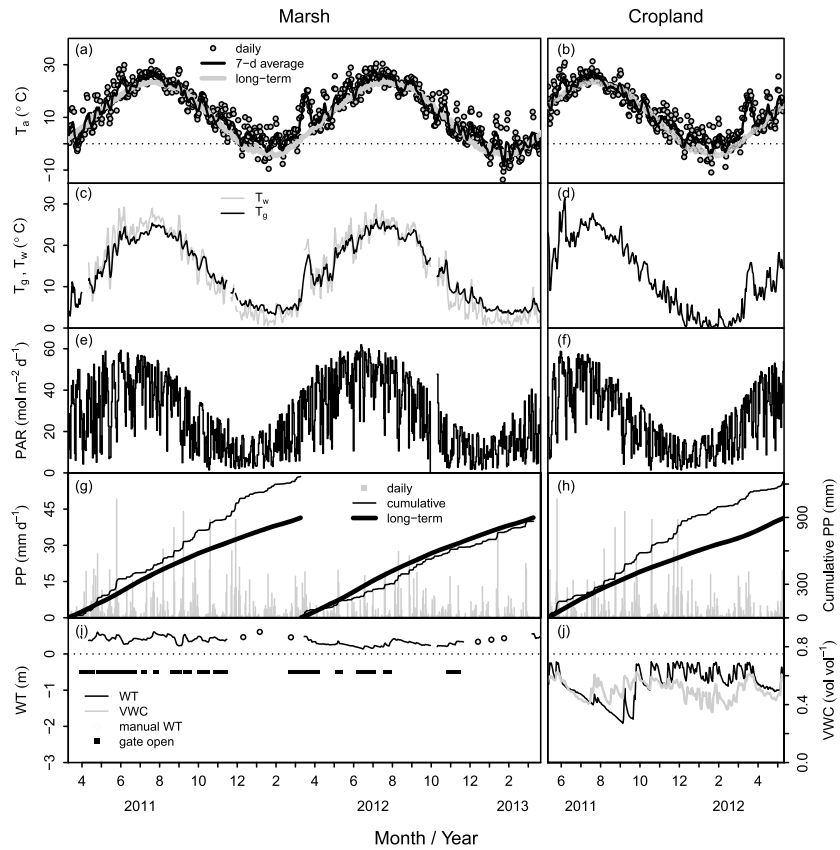


Figure 2. Time series of the daily micrometeorological variables at the marsh and cropland sites, including (a, b) air temperature (T_a , grey circles), (c, d) soil temperature (T_g , black lines) and surface water temperature (T_w , grey lines), (e, f) photosynthetically active radiation (PAR, black lines), (g, h) precipitation (PP, grey bars), and (i) groundwater level (WT, black lines) and (j) volumetric soil water content (VWC, grey lines). Seven day moving average and long-term (1893–2013) average T_a are shown as black and grey solid lines in Figures 2a and 2b. Annual cumulative PP and long-term (1893–2013) average cumulative PP are shown as solid and thick lines in Figures 2g and 2h. Dates with the outflow gate open at the marsh are marked as closed squares in Figure 2i. The average sediment (soil) surface near the tower was taken as the reference level (0) of the WT measurement and positive WT indicated the water level above the ground. The water level sensor was removed from the marsh site during ice-covered winter; hence, no continuous data were available in those periods. Manual WT measurements in the winter are marked as open circles in Figure 2i.

2.7. Statistical Analysis

All of the statistical tests and model fittings were conducted with the R language (R Development Core Team, 2013, version 3.0.0). The parameter estimation in the F_{CO_2} partitioning was conducted using the “nlreg” package [Bellio and Brazzale, 2003]. The univariate and multiple linear regressions were conducted using the “lm” function. The correlations among variables were examined using the “cor” function. Unless specified, the significance level was set to 0.05 and the uncertainty (\pm) always referred to 95% confidence intervals in the following sections.

3. Results

3.1. Micrometeorology and Hydrology

The years 2012 and 2011 were recorded as the second and third warmest (2.1°C and 1.9°C higher than the long-term average of 10.0°C) over the last 118 years in the region (Figures 2a and 2b and Table S3). The 2011 winter (December 2011 to February 2012) was exceptionally warm (Figure 2a). In total, there were only 29 days that had daily air temperature below 0°C, much fewer than 59 days in the 2012 winter. The warm 2011 winter was followed by warmer spring temperature on 11–25 March 2012. Air temperature increased drastically to ~20°C during this early spring period and was much higher than the long-term average of ~4°C.

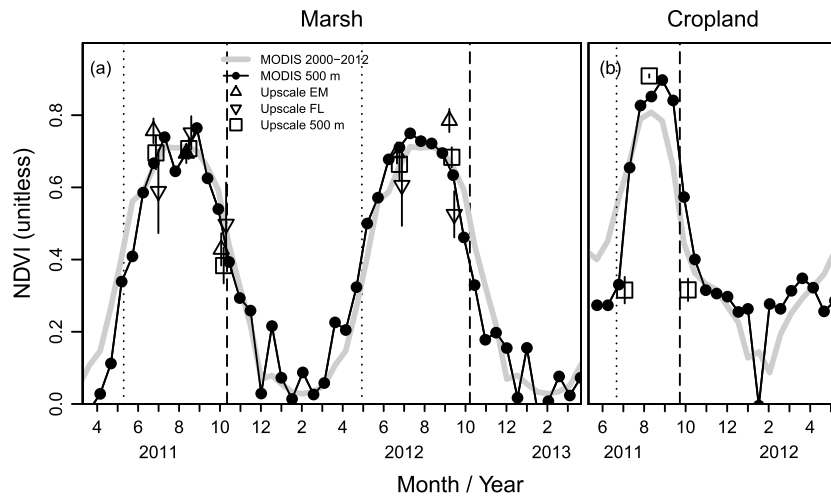


Figure 3. Sixteen day normalized difference vegetation index (NDVI, MOD13Q1, closed circles and black lines) obtained from the Moderate Resolution Imaging Spectroradiometer with a $500 \times 500 \text{ m}^2$ spatial extent at the (a) marsh and (b) cropland sites. Multiyear averages from 2000 to 2012 are shown as grey lines. Upscale $500 \times 500 \text{ m}^2$ NDVI (open squares) from in situ point-sampled reflectance measurements (ASD multispectrometer) are marked with 95% confidence intervals (vertical black segments) (see Text S1 for details). Upscale NDVI for the emergent vegetation (open triangles) and floating-leaved vegetation (reversed open triangles) areas at the marsh site are also presented. Dotted lines and dash lines indicate the start and end of the growing season as determined by the first and last three consecutive days with daily gross ecosystem production larger than $1 \text{ g C-CO}_2 \text{ m}^{-2} \text{ d}^{-1}$.

Despite the similarity in atmospheric climate conditions (e.g., air temperature, PAR), soil temperature showed slightly different patterns between the two sites. In general, the marsh site had higher winter soil temperature and lower summer soil temperature than the cropland site (Figures 2c and 2d).

In addition, 2011 had an extremely high amount of annual precipitation ($\sim 372 \text{ mm}$ higher than the long-term average of 897 mm) (Figures 2g and 2h and Table S3). The marsh manager opened the water outflow gate several times throughout the summer and fall in 2011 in order to maintain the water level at $0.2\text{--}0.6 \text{ m}$ above the ground surface (Figure 2i). The warm winter in 2011 had the majority of precipitation as rainfall instead of snowfall. Groundwater was continuously recharged at the cropland site. Hence, groundwater level was high around $0.2\text{--}0.8 \text{ m}$ beneath the ground surface (Figure 2j). The 2012 summer was dry compared to 2011 and the long-term average. Groundwater level was continuously drawn down from late May to late July and from early August to October at the marsh and the outflow gate was kept closed throughout most of the late summer and fall (Figure 2i).

3.2. Satellite-Based Vegetation Characteristics

The NDVI showed spring green-up roughly 16 days later and 4 days earlier than the multiyear average (2000–2012) in 2011 and 2012 at the marsh (Figure 3a), respectively. Additionally, NDVI declined around 16 days earlier in the fall of 2012 at the marsh. The multiyear average showed that NDVI increased quickly after May at the marsh, peaked between mid-July and mid-August, and declined quickly after September. In 2012, green-up occurred earlier with peak NDVI on 11 July. In contrast, the delayed green-up in 2011 led to a late peak NDVI on 29 August. The multiyear average showed that NDVI increased after June and peaked in August at the cropland (Figure 3b). NDVI declined quickly after crop harvesting in late September. In 2011, NDVI showed an 8 day delay in the spring green-up and the fall decline in comparison with the multiyear average at the cropland. The delay was attributed to the postponed crop planting and harvest caused by the extremely high precipitation and near-saturated soil water content in May (Figures 2h and 2j).

3.3. Seasonal Variability in F_{CO_2}

While the marsh had 155 and 162 days of growing seasons in 2011 (12 May to 12 October) and 2012 (30 April to 7 October) (Figure 4c), respectively, the cropland had 94 days in 2011 (23 June to 23 September). The temporal shift of growing season between years corresponded to the interannual differences in the NDVI dynamics (Figure 3a). Overall, the start and end of the growing season occurred in correspondence with NDVI

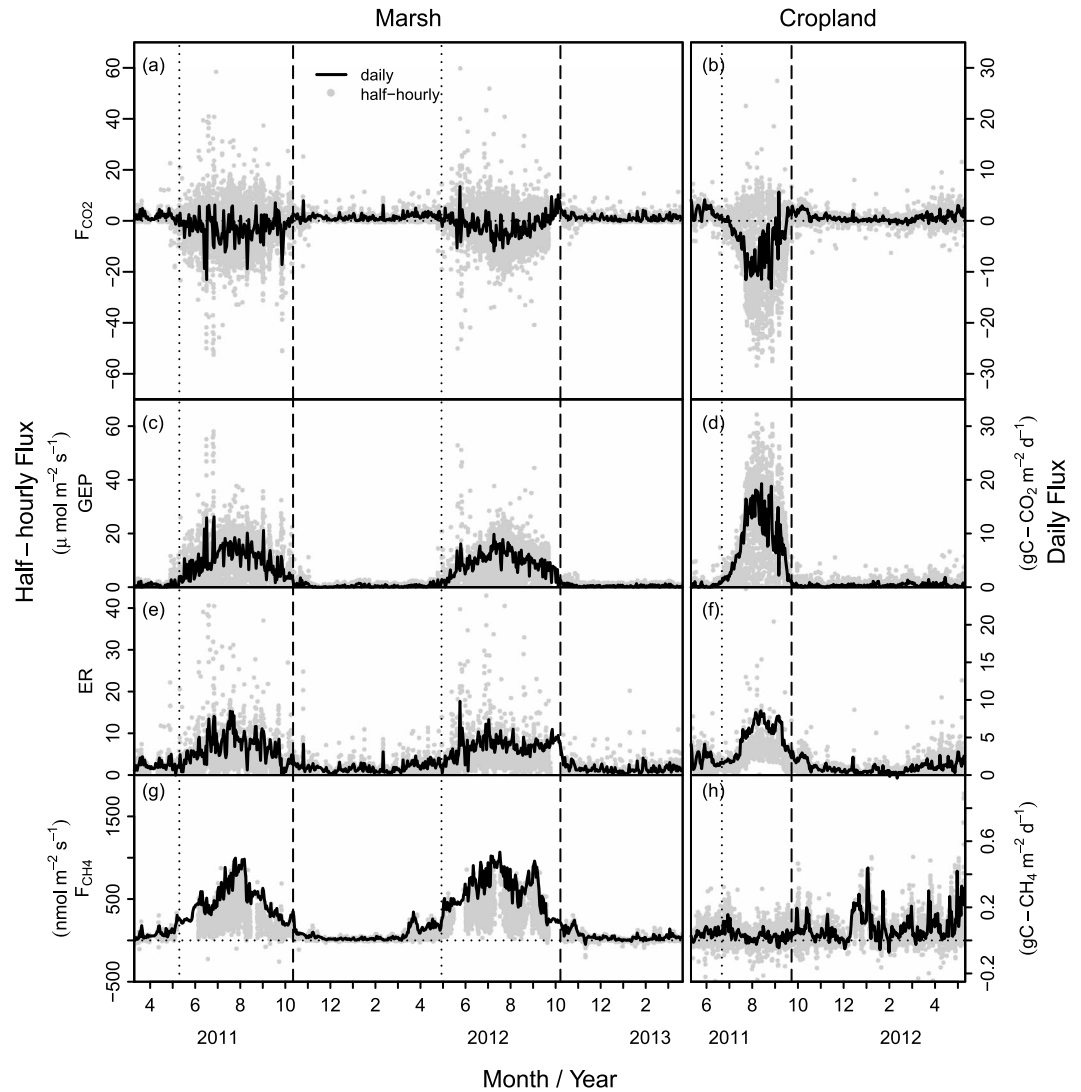


Figure 4. Time series of half-hourly (grey circles) and daily (solid lines) fluxes at the marsh and cropland sites, including (a, b) net ecosystem CO₂ exchange (F_{CO_2}), (c, d) gross ecosystem production (GEP), (e, f) ecosystem respiration (ER), and (g, h) net ecosystem CH₄ exchange (F_{CH_4}). Half-hourly data were not gap filled and daily data were integrated from gap-filled half-hourly data by the marginal distribution sampling method. F_{CH_4} was much smaller at the cropland; hence, the daily and half-hourly F_{CH_4} were presented in a tenfold scale in Figure 4h. Dotted and dashed lines indicate the start and end of the growing season as determined by the first and last three consecutive days with daily GEPs larger than $1 \text{ g C-CO}_2 \text{ m}^{-2} \text{ d}^{-1}$.

around 0.36–0.40 at the marsh. The growing season started and ended while NDVI was ~ 0.36 and ~ 0.69 at the cropland site (Figures 3b and 4d).

Both the marsh and cropland sites showed strong seasonality in F_{CO_2} , GEP, and ER (Figure 4). After the snowmelt in the spring, the marsh and cropland acted as sources of CO₂. From 12 May to the start of growing season, the cumulative F_{CO_2} was $72.9 \pm 11.4 \text{ g C-CO}_2 \text{ m}^{-2}$ at the cropland site. The cropland turned into a CO₂ sink around 3 July, 10 days after the start of growing season, and remained a sink through most of the growing season (Figure 4b). The cumulative F_{CO_2} , GEP, and ER in the growing season were -371.7 ± 35.1 , 933.2 ± 30.7 , and $561.5 \pm 36.2 \text{ g C-CO}_2 \text{ m}^{-2}$ (Table S4), respectively. Noticeably, there were several intense rainfall events ($>15 \text{ mm d}^{-1}$) in the late growing season (Figure 2h). During these rainy periods, GEP was largely reduced and cropland turned to a CO₂ source (Figures 4b and 4d). After mid-September, cropland acted again as a CO₂ source and the daily F_{CO_2} (ER) was $1.9 \pm 0.5 \text{ g C-CO}_2 \text{ m}^{-2} \text{ d}^{-1}$ before the harvest on

23 October (Figures 4b and 4f). The F_{CO_2} (ER) decreased quickly after the harvest and remained around 0.3 ± 0.1 g C-CO₂ m⁻² d⁻¹ throughout the winter.

F_{CO_2} and ER at the marsh, in contrast, showed more fluctuations within the seasonal trend than those at the cropland site (Figures 4a and 4e). From 12 March to the start of growing season, the cumulative F_{CO_2} (ER) was 53.7 ± 6.7 and 54.2 ± 3.8 g C-CO₂ m⁻² in 2011 and 2012, respectively. The marsh generally acted as a CO₂ sink after the start of growing season. However, occasional but evident CO₂ efflux still occurred through the growing season (Figure 4a). Those days with positive daily F_{CO_2} occurred mostly 1–3 days after the large rainfall events (>15 mm d⁻¹). For example, there were several intense rainfall events between 18 and 23 July 2011 with a cumulative precipitation of 125 mm (Figure 2g). The marsh quickly turned into a net CO₂ source and released ~3 g C-CO₂ m⁻² to the atmosphere within 6 days (Figure 4a). In the same period, the cumulative GEP and ER were 40.7 ± 3.6 and 43.7 ± 3.6 g C-CO₂ m⁻², respectively. In comparison to the previous (12–17 July) and the following 6 days (24–29 July), the difference of F_{CO_2} resulted mostly from the enhanced ER, which was 10.9–18.7 g C-CO₂ m⁻² higher in this rainy period. GEP, in contrast, only declined marginally to 1.0–3.0 g C-CO₂ m⁻² due to the reduced incident radiation. As the temperature was lower in the rainy period, the enhanced ER was most likely caused by the high decomposition after the pulsed hydrological input of organic matter and nutrients from nearby agricultural ditches. Throughout the growing seasons, the cumulative F_{CO_2} , GEP, and ER were -212.0 ± 47.4 , 812.5 ± 30.5 , and 600.5 ± 48.4 g C-CO₂ m⁻² in 2011 and -116.7 ± 51.3 , 787.9 ± 32.8 , and 671.2 ± 52.3 g C-CO₂ m⁻² in 2012 (Table S4). After the end of growing season, F_{CO_2} (ER) declined from ~1.1 to ~0.5 g C-CO₂ m⁻² d⁻¹ in early December when the surface water started to freeze at the marsh site (Figures 4a and 4e). Through the winter, F_{CO_2} (ER) was low and remained around 0.5 ± 0.1 and 0.4 ± 0.1 g C-CO₂ m⁻² d⁻¹ in 2011 and 2012, respectively.

3.4. Seasonal Variability in F_{CH_4}

F_{CH_4} at the marsh site showed strong seasonality and followed closely the seasonal temperature dynamics (Figures 2a, 2c, and 4g). Positive F_{CH_4} was observed throughout the majority of the study period at the marsh site. F_{CH_4} increased quickly following the rising temperature in early March. For example, the early warm-up during 11–25 March 2012 resulted in the daily F_{CH_4} increasing from 0.02 g C-CH₄ m⁻² d⁻¹ on 10 March (air and soil temperature: 2.6°C and 6.3°C) to 0.20 g C-CH₄ m⁻² d⁻¹ on 23 March (air and soil temperature: 15.6°C and 17.6°C) (Figure 4g). From 12 March to the start of growing season, the cumulative F_{CH_4} was 2.9 ± 0.4 and 4.8 ± 0.6 g C-CH₄ m⁻² in 2011 and 2012, respectively. After the start of growing season, F_{CH_4} increased continuously and peaked around 0.60 g C-CH₄ m⁻² d⁻¹ on 25 July in 2011 and on 8 July in 2012. Interestingly, F_{CH_4} showed a quick decline with the decreasing temperature after mid-July in 2012. While the daily air and soil temperature dropped to the local minimum of 19.8°C and 20.4°C on 11 August, the daily F_{CH_4} decreased to 0.25 g C-CH₄ m⁻² d⁻¹. After that, air and soil temperature increased gradually back to 25.5°C and 23.5°C on 3 September and the daily F_{CH_4} increased to 0.54 g C-CH₄ m⁻² d⁻¹. Throughout the growing season, the cumulative F_{CH_4} was 37.1 ± 4.1 and 49.2 ± 4.9 g C-CH₄ m⁻² in 2011 and 2012, respectively. The daily F_{CH_4} dropped quickly after the surface water was frozen in early December and kept low around 0.01 g C-CH₄ m⁻² d⁻¹ through most of the winter (Figure 4g).

The F_{CH_4} at the cropland site showed weak seasonality and dependency on the temperature dynamics. Most notably, F_{CH_4} was much smaller at the cropland site than that at the marsh (Figure 4h, presented in a tenfold scale). Generally, F_{CH_4} was minor throughout the growing season, with an average daily flux of 0.003 g C-CH₄ m⁻² d⁻¹, which was even lower than that in the winter at the marsh. Surprisingly, F_{CH_4} increased slightly after the end of growing season and occasionally rose to 0.02–0.03 g C-CH₄ m⁻² d⁻¹ in the winter. The causes of the enhanced F_{CH_4} in the cold winter were not clear. Most days with rising F_{CH_4} had higher wind speeds and were 1–2 days after intense rainfall events and increasing temperatures. For example, there was 15, 12, and 13 mm cumulative precipitation during 14–15, 20–22, and 30–31 December in 2011 (Figure 2h), respectively. These days had a 7–10°C increase in air temperature and a 3–6°C increase in soil temperature from their precedent days. The daily F_{CH_4} increased to ~0.02, ~0.03, and ~0.04 g C-CH₄ m⁻² d⁻¹ during 15–16 December, 21–23 December, and 2–3 January (Figure 4h), respectively, which was 1–2 days after the warm and rainy days. The daily wind speed was generally higher (3.4–7.1, 2.3–4.4, and 4.4–6.0 m s⁻¹) on these F_{CH_4} -enhanced days. As the precedent rainfall, rising temperature, and wind speed partially explained daily F_{CH_4} increase, there were days having similar weather but showing only minor daily F_{CH_4} (e.g., 23–25

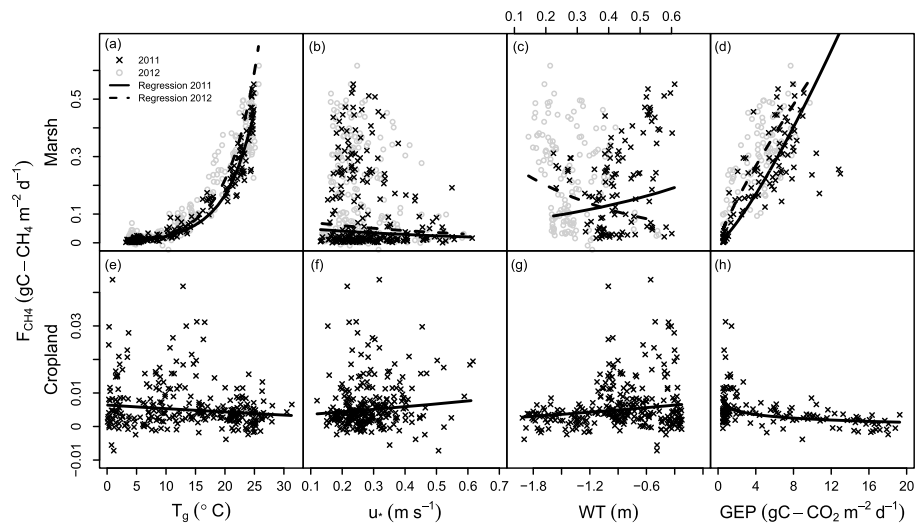


Figure 5. Regression models of the daily net ecosystem CH₄ exchange (F_{CH_4}) against (a, e) soil temperature (T_g), (b, f) friction velocity (u_*), (c, g) groundwater table (WT), and (d, h) and gross ecosystem production (GEP). Marsh data are grouped into 2011 (black crosses) and 2012 (grey circles) and separate model parameters are fitted for 2011 (solid lines) and 2012 (dashed lines). Model formula and statistics are provided in the supporting information (Table S5).

November, 30 November to 2 December). From December 2011 to February 2012, the cumulative F_{CH_4} was 0.8 ± 0.2 g C-CH₄ m⁻².

3.5. Regulation of F_{CH_4}

The daily F_{CH_4} may be explained mostly by soil temperature at the marsh ($p < 0.001$, $R^2 = 0.86$) (Figure 5a and Table S5). The daily F_{CH_4} increased roughly 20% for every 1°C increase in the daily soil temperature and the temperature sensitivities were not significantly different between 2011 and 2012 (Table S5). Both groundwater level and u_* explained only minor variations in the daily F_{CH_4} at the marsh ($R^2 = 0.04$ and 0.02) (Figures 5b and 5c and Table S5). After eliminating the confounding effects of soil temperature, u_* only explained an additional 1% of variation in the daily F_{CH_4} and groundwater level became insignificant (Table S5). For the cropland site, none of the physical factors (soil temperature, u_* , and groundwater level) explained more than 5% of the variations in the daily F_{CH_4} (Figures 5e–5g and Table S5).

Interestingly, the daily F_{CH_4} was highly correlated with the daily GEP at the marsh site even after eliminating the confounding effects of soil temperature (Table S5). Our multiple linear regression analyses showed that the parameters of soil temperature (0.18, $p < 0.001$) and GEP (0.85, $p < 0.001$) were both significant. There was significant interaction between soil temperature and GEP (-0.03 , $p < 0.001$; Table S5), and thus, the enhancing effects of soil temperature and GEP partially compensated each other while both soil temperature and GEP increased. For the cropland site, as F_{CH_4} tended to be higher during the nongrowing season, F_{CH_4} increased slightly as GEP decreased ($R^2 = 0.14$, $p < 0.001$; Figure 5h and Table S5).

The regulation of soil temperature became less relevant when examining the short-term (half-hourly to weekly) dynamics of F_{CH_4} at the marsh (Figures 6 and S1). S_{Tg} , the short-term soil temperature sensitivity, was found to be significant in only forty-one 8 day periods (53%) and ranged largely from 16 to -20 (Figure 6c). After discarding the periods with negative S_{Tg} , there were only 26 periods (34%) that had significantly positive S_{Tg} . Unexpected negative and large S_{Tg} occurred mostly in the hottest periods in the summer and the coldest periods in the winter. During these periods, the temperatures reached the local maximum (or minimum) and soil temperature was nearly stable. For example, soil temperature reached the local maximum and remained around 23–25°C from 25 July to 1 August 2011 (Figure 7b). Surprisingly, F_{CH_4} showed an evident diurnal pattern fluctuating from 100 to 1200 nmol m⁻² s⁻¹ regardless of the stable soil temperature (Figures 7a and 7b).

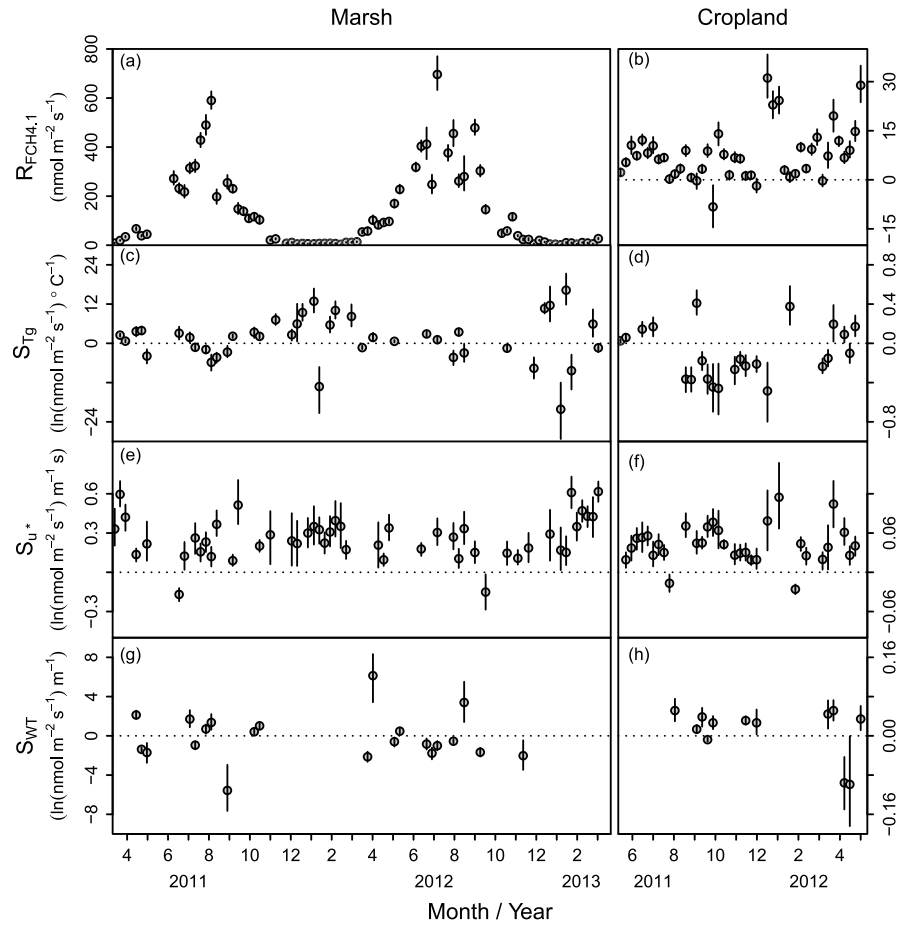


Figure 6. Model parameters of the multiple linear regression against half-hourly net ecosystem CH₄ exchange (F_{CH_4}) at the (a, c, e, g) marsh and (b, d, f, h) cropland sites. Each point represents a model parameter estimation obtained from an 8 day nonoverlapping period. There were 91 and 45 periods for the marsh and cropland sites, respectively, within which 77 and 44 periods had enough data ($N > 48$) for model estimation. For each period, the model was simplified by eliminating the insignificant parameters and only the least adequate models are presented here. Model formulas are listed in the main text (section 2.4 and equation (1)). $R_{FCH_4,1}$ is the base F_{CH_4} ($\text{nmol m}^{-2} \text{s}^{-1}$) at the period-averaged soil temperature (T_g), friction velocity (u^*), and groundwater table (WT). S_{Tg} , S_{u^*} , and S_{WT} represent the sensitivities of F_{CH_4} to every 10°C change in T_g , every 0.1 m s^{-1} change in u^* , and every 0.1 m change in WT , respectively. Vertical segments indicate the 95% uncertainty intervals of the parameter estimation.

Turbulent mixing was more relevant in regulating the short-term than long-term dynamics of F_{CH_4} . The half-hourly F_{CH_4} at the marsh showed evident dependency on u^* in 58% of the 8 day periods (Figures 6e and S1). On the other hand, there were 30 periods that had insignificant S_{u^*} . The bimodal S_{u^*} (either positive or zero) suggested that turbulent mixing was crucial only in periods when F_{CH_4} was dominantly limited by the transport processes. For example, the frozen ice thawed after several days of rising air temperature from 18 to 20 January 2013 (Figures 8b and 8c). F_{CH_4} increased quickly to $\sim 150 \text{ nmol m}^{-2} \text{s}^{-1}$ while u^* reached up to 0.8 m s^{-1} on 20 January. Over the 8 days, half-hourly F_{CH_4} fluctuated greatly from 0 to $150 \text{ nmol m}^{-2} \text{s}^{-1}$ while soil temperature was stable with minor fluctuation ($\pm 1^\circ\text{C}$). The decoupling of soil temperature and F_{CH_4} suggested that F_{CH_4} was primarily regulated by the transport of CH_4 in these winter periods. As the marsh site maintained inundation with slightly fluctuating groundwater level, the groundwater level was found to be irrelevant in explaining the dynamics of F_{CH_4} in most of the periods (Figures 6g and S1). Overall, there were only 21 periods with significant short-term groundwater level sensitivity (S_{WT}).

We found that half-hourly F_{CH_4} was coupled with air temperature/VPD in most of the periods in the growing season (Figures 7 and S2). S_{T_a} (i.e., the short-term air temperature sensitivity) and S_{VPD} (i.e., the short-term VPD sensitivity) were found significant (i.e., $\neq 0$) in 17 (59%) and 10 (37%) periods in the growing season

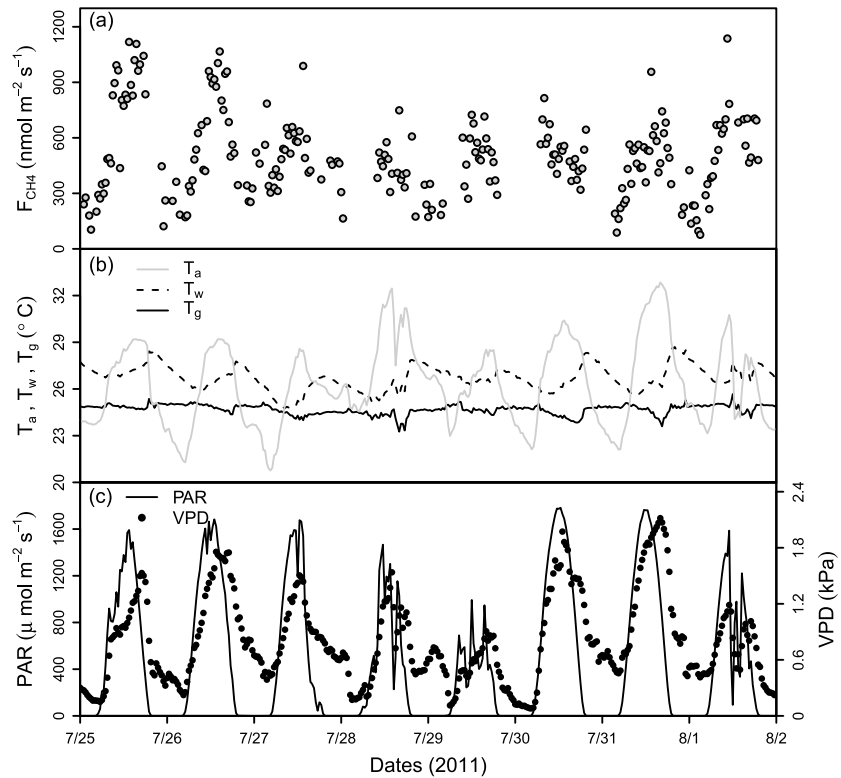


Figure 7. Time series of (a) half-hourly net ecosystem CH₄ exchange (F_{CH_4} , grey circles), (b) soil temperature (T_g , black lines), surface water temperature (T_w , dashed lines), and air temperature (T_a , grey lines), and (c) photosynthetically active radiation (PAR, black lines) and vapor pressure deficit (VPD, black circles) at the marsh site. Data were from 25 July to 1 August 2011. F_{CH_4} was not gap filled.

(Figures S2b and S2c). Most of the significant S_{T_a} and S_{VPD} occurred between mid-June and mid-September, during which NDVI was high and the vegetation canopy was fully developed (Figure 3a). The average S_{T_a} was 0.83 and 0.62 in 2011 and 2012 while the average S_{VPD} was 0.04 and 0.05, respectively.

For the cropland site, there was no apparent seasonality in $R_{F_{CH_4,1}}$ or S_{T_g} , suggesting that soil temperature was not the dominant factor in regulating the short-term F_{CH_4} (Figures 6b and 6d). S_{u^*} showed a bimodal pattern (positive or zero) analogous to that at the marsh site (Figures 6e and 6f), which revealed the importance of turbulent mixing in regulating the CH₄ transport in certain periods. On the other hand, there were 12 periods (27%) that had significant groundwater level sensitivity (S_{WT_i} ; Figure 6h).

3.6. Annual Atmospheric Carbon Budget

F_{CH_4} contributed a significant portion to the annual atmospheric carbon budget at the marsh (Table S4). Two year average annual F_{CH_4} ($49.7 \text{ g C-CH}_4 \text{ m}^{-2} \text{ yr}^{-1}$) from the marsh was higher than average annual net CO₂ uptake ($-21.0 \text{ g C-CO}_2 \text{ m}^{-2} \text{ yr}^{-1}$). On an annual basis, GEP sequestered 812.5 ± 30.5 and $787.9 \pm 32.8 \text{ g C-CO}_2 \text{ m}^{-2}$ in 2011 and 2012, respectively, while ER released 741.8 ± 64.9 and $816.6 \pm 69.9 \text{ g C-CO}_2 \text{ m}^{-2}$ back to the atmosphere. The annual F_{CO_2} was $-70.6 \pm 63.9 \text{ g C-CO}_2 \text{ m}^{-2}$ (a CO₂ sink) in 2011. Surprisingly, ER was compatible with GEP in the extremely warm 2012 and led to an annual CO₂ budget of $28.7 \pm 68.9 \text{ g C-CO}_2 \text{ m}^{-2}$ (near-CO₂ neutral). Annual F_{CH_4} was 42.3 ± 4.9 and $57.0 \pm 6.1 \text{ g C-CH}_4 \text{ m}^{-2}$ in 2011 and 2012, respectively. In total, F_{CH_4} compensated a large portion of F_{CO_2} and led to a near-neutral ($-28.3 \pm 64.1 \text{ g C m}^{-2}$) atmospheric carbon budget at the marsh in 2011. For the extremely warm 2012, the marsh acted as an atmospheric carbon source ($85.7 \pm 69.2 \text{ g C m}^{-2}$) after considering the contribution of F_{CO_2} and F_{CH_4} . Despite the large interannual variation in F_{CO_2} and F_{CH_4} , CH₄ accounted for a significant portion in the atmospheric carbon budget of the marsh.

The cropland site, in contrast, was an atmospheric carbon sink with or without considering the contribution of CH₄ (Table S4). The annual GEP and ER were 933.2 ± 30.7 and $781.4 \pm 75.5 \text{ g C-CO}_2 \text{ m}^{-2}$

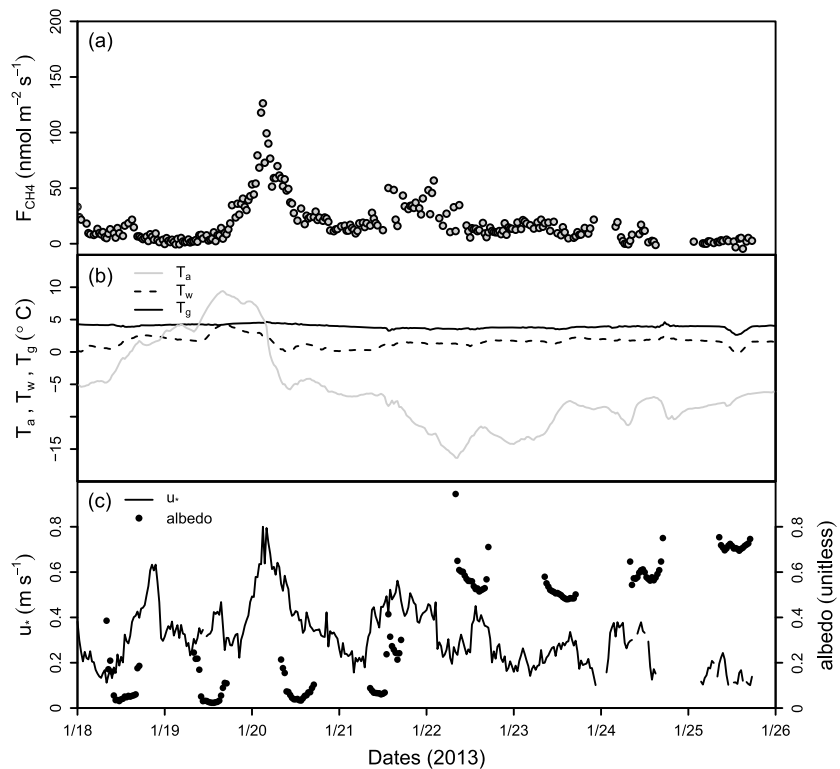


Figure 8. Time series of (a) half-hourly net ecosystem CH₄ exchange (F_{CH_4} , grey circles), (b) soil temperature (T_g , black lines), surface water temperature (T_w , dashed lines), and air temperature (T_a , grey lines), and (c) friction velocity (u_* , black lines) and albedo (closed circles) at the marsh site. Data were from 18 to 25 January 2013. F_{CH_4} was not gap filled. Albedo is adopted to indicate the periods with frozen ice/snow cover (albedo > 0.2) in contrast to periods with open water (albedo < 0.2).

and led to a CO₂ sink of -151.8 ± 74.4 g C-CO₂ m⁻². The atmospheric carbon budget changed slightly to -149.5 ± 74.5 g C m⁻² after considering the contribution of CH₄ (2.3 ± 1.1 g C-CH₄ m⁻²).

4. Discussion

4.1. Physical Regulation of F_{CH_4} at the Marsh

Soil temperature, groundwater level, and u_* are the most frequently used environmental factors in modeling ecosystem-scale F_{CH_4} [Hatala et al., 2012; Herbst et al., 2013; Olson et al., 2013; Tagesson et al., 2012]. These factors represent, although implicitly, the regulation of CH₄ production, oxidation, and transport [Le Mer and Roger, 2001]. We found that these factors are also relevant in explaining the F_{CH_4} dynamics at the marsh, although different factors may regulate F_{CH_4} at different temporal scales. Soil temperature, highly associated with methanogenesis activity and the production of CH₄ [Le Mer and Roger, 2001], was the major controlling factor of the daily-to-yearly F_{CH_4} . The regulation of seasonal F_{CH_4} by soil temperature was also reported in the previous studies [Hanis et al., 2013; Herbst et al., 2013; Tagesson et al., 2012]. The high R^2 and similar temperature sensitivity between 2011 and 2012 suggested a relatively stable seasonal temperature dependency at the marsh.

Considering the short-term (half-hourly to weekly) F_{CH_4} dynamics, however, soil temperature was irrelevant and regulation of transport became the major limiting factor of F_{CH_4} . At the half-hourly to weekly scale, u_* became more relevant than at the daily-to-yearly scale, suggesting that transport was more important in regulating the short-term F_{CH_4} dynamics [Hargreaves and Fowler, 1998; Herbst et al., 2011b]. The importance of u_* should be noted especially in the nongrowing season when live macrophytes are absent and diffusion and ebullition become the dominant pathways for CH₄ transport. As shown in the selected wintertime series (Figure 8), a short ice-thawing period accompanied by strong turbulence conditions led to a drastic

increase in F_{CH_4} , even when soil temperature remained steady. The importance of turbulent mixing in enhancing CH_4 emission after ice breakup was also highlighted in a previous study [Lundin *et al.*, 2013], which reported that the CH_4 emission during periods after ice breakup accounted for ~45% of the annual CH_4 emission at subarctic lakes. On the other hand, plant-modulated gas flow played an important role in facilitating the outgassing of CH_4 , especially in the peak growing season. The half-hourly F_{CH_4} followed closely the diurnal changes of air temperature and VPD. We believe that the half-hourly F_{CH_4} is largely driven by the pressurized ventilation of the aquatic macrophytes, which was documented to be controlled mainly by air temperature and VPD [Dacey, 1981; Grosse, 1996; Richards *et al.*, 2012] (see section 4.2. for details).

Groundwater level accounted for a minor portion in explaining both the seasonal and diurnal F_{CH_4} . Groundwater level represented the regulation of the CH_4 production/oxidation balance through the varying depths of anaerobic and aerobic zones in the soil [Whalen, 2005]. The irrelevance of groundwater level was noted in some previous studies [e.g., Jackowicz-Korczyński *et al.*, 2010; Rinne *et al.*, 2007; Wille *et al.*, 2008] where the sites were permanently inundated or groundwater level only fluctuated slightly. The marsh site has been managed as inundated in the past decade. Hence, groundwater level is irrelevant in explaining the F_{CH_4} dynamics over the 2 year study period. However, it should be noted that the permanently inundated and consequently anaerobic conditions in the sediments are definitely the prerequisites for generating such a high amount of CH_4 at the marsh site.

4.2. Plant Modulation of F_{CH_4} at the Marsh

Plants modulated F_{CH_4} mainly through facilitating CH_4 transport from the sediment to the atmosphere at the marsh. While the daily F_{CH_4} followed closely with the seasonality of soil temperature, the half-hourly F_{CH_4} showed an evident diurnal pattern following closely with air temperature and VPD in the peak growing season. A similar pattern was documented in a temperate marsh dominated by *Phragmites australis* by Kim *et al.* [1999]. They found that the diurnal change of F_{CH_4} is driven by the convective gas flow through *P. australis*. The plant-modulated gas flow is more efficient in transporting CH_4 to the atmosphere than the diffusion through the water column.

Dacey and Klug [1979] and Dacey [1981] addressed that floating-leaved vegetation, such as the yellow water lily (*Nuphar luteum*), constituted a pressurized throughflow system that greatly enhanced gas transport in plants. Since then, subsequent studies explored this “pressurized ventilation” across a variety of aquatic floating-leaved plants, such as *Nymphaea*, *Nuphar*, and *Nelumbo* [Dacey and Klug, 1979; Grosse, 1996; Grosse *et al.*, 1991, 1996; Richards *et al.*, 2012; Sebacher *et al.*, 1985], and emergent plants, such as *Typha*, *Cyperus*, and *Phragmites* [Bendix *et al.*, 1994; Brix *et al.*, 1992; Sebacher *et al.*, 1985; Whiting and Chanton, 1996]. Despite the slight structural differences in the ventilation system among species, the convective throughflow is believed to be generated by the internal pressurization [Brix *et al.*, 1992; Dacey, 1981; Grosse, 1996; Tornberg *et al.*, 1994]. Briefly, air enters the young or middle-aged leaves as a result of the temperature and/or humidity gradient between the atmosphere and the lacunae of leaves. The entry of excess air leads to higher pressure inside the leaves and forces air to be convected down along the petioles (floating-leaved plants) or lacunae (emergent plants) to the rhizomes. Air is then vented back through the old shoots or leaves to the atmosphere. While the plants benefit by transporting sufficient oxygen from the atmosphere to their submerged parts, CH_4 enters the plant roots from the sediment and passes rapidly through the plants to the atmosphere.

The dominant aquatic macrophytes—water lilies and narrow-leaved cattails—at our marsh site have been noted for their physiological capabilities to facilitate the CH_4 outgassing [Grosse, 1996; Schipper and Reddy, 1994; Sebacher *et al.*, 1985; Tornberg *et al.*, 1994]. It was documented that the leaf-specific gas flow rates can reach up to 4.2 and 1.9 mL cm⁻² h⁻¹ from water lilies [Grosse *et al.*, 1996] and narrow-leaved cattails [Tornberg *et al.*, 1994], respectively. Sebacher *et al.* [1985] documented that rooted aquatic macrophytes (i.e., emergent or floating-leaved plants) had generally higher leaf CH_4 emission rates than un-rooted plants. Among the 16 varieties of aquatic plants that have been tested, water lily and cattail (*Typha latifolia*) had the highest plant-specific CH_4 emissions of 0.014 and 0.007 g C- CH_4 d⁻¹, respectively. Schipper and Reddy [1994] addressed that the F_{CH_4} mediated by water lily (0.08–0.65 g C- CH_4 m⁻² d⁻¹) was much higher than the background diffusive F_{CH_4} (0.01 g C- CH_4 m⁻² d⁻¹) at the Everglades and the Okefenokee Swamp in Florida. Similarly, the F_{CH_4} mediated by cattail (*Typha* sp.) (0.08–1.05 g C- CH_4 m⁻² d⁻¹) was much higher than the

background diffusive F_{CH_4} ($0.01 \text{ g C-CH}_4 \text{ m}^{-2} \text{ d}^{-1}$) [Schipper and Reddy, 1994]. In sum, as CH_4 continues to be generated at the permanently inundated marsh site, the cattail and water lily play key roles in ventilating CH_4 quickly from the sediments to the atmosphere. The plant-modulated gas flow is more efficient in transporting CH_4 than the diffusion through the water column. Additionally, the gas flow bypasses the aerobic zone in the water column and consequently keeps CH_4 from being oxidized [Whalen, 2005].

It has been noted that plants can also facilitate CH_4 production through supplementing photosynthate as root exudate into the rhizosphere [Dacey, 1981; Dorodnikov et al., 2011; King et al., 2002; Ström et al., 2012]. Our results showed that the daily F_{CH_4} was correlated with the daily GEP at the marsh site and the correlation was not caused by the confounding effects of soil temperature. However, while GEP was also highly correlated with PAR and air temperature (i.e., the driving factors of the pressurized ventilation [Dacey, 1981; Grosse, 1996]), it is difficult to separate the supplementing effect from the ventilating effect based on our current research design. To date, there are only a few studies that traced the source of $\text{CH}_4\text{-C}$ in the field [e.g., Chanton et al., 2008; Dorodnikov et al., 2011; King et al., 2002]. We argue that further research on this topic is needed, especially to discriminate the underlying mechanisms of the correlated F_{CH_4} and GEP, in order to better understand the role of plant modulation in wetland CH_4 processes.

4.3. Annual Atmospheric Carbon Budget

The annual F_{CH_4} at the marsh is relatively high in comparison to the reported freshwater wetlands in North America [Bridgham et al., 2006]. Bridgham et al. [2006] synthesized the field measurements of wetland F_{CH_4} in North America and reported that the geometric and arithmetic means of the annual F_{CH_4} are 5.7 and $27.0 \text{ g C-CH}_4 \text{ m}^{-2} \text{ yr}^{-1}$ in freshwater wetlands. While the majority of the reported wetlands (68%) have relatively low annual F_{CH_4} ($< 25 \text{ g C-CH}_4 \text{ m}^{-2} \text{ yr}^{-1}$), there are a few wetlands that have exceptionally high annual F_{CH_4} , up to $100\text{--}170 \text{ g C-CH}_4 \text{ m}^{-2} \text{ yr}^{-1}$. The wide range of reported annual F_{CH_4} reflects the fact that wetlands are greatly diverse in their vegetation composition, hydrology, and soil conditions. As discussed in the previous sections, we believe that the permanent inundation and plant-modulated gas flow are the major causes for such a large amount of CH_4 emission at the marsh. To date, few wetland studies have quantified the annual F_{CH_4} in freshwater marshes (Table S6). The reported annual F_{CH_4} ranges between 14 and $132 \text{ g C-CH}_4 \text{ m}^{-2} \text{ yr}^{-1}$, with a mean of $53 \text{ g C-CH}_4 \text{ m}^{-2} \text{ yr}^{-1}$. These freshwater marshes, characterized by deep water and long-lasting inundation conditions, are dominated by emergent and/or floating-leaved macrophytes. The majority of the macrophytes, such as *Typha*, *Cyperus*, *Phragmites*, *Pontederia*, *Nymphaea*, *Nuphar*, and *Nelumbo*, possess pressurized ventilation characteristics [Brix et al., 1992; Dacey and Klug, 1979; Grosse, 1996; Grosse et al., 1991; Richards et al., 2012; Tornberg et al., 1994]. Consequently, CH_4 emission is clearly high in these (mostly) temperate zone freshwater marshes.

In comparison with the limited reports of annual F_{CH_4} and F_{CO_2} at temperate wetlands, our marsh site has exceptionally high F_{CH_4} contribution to the atmospheric carbon budget (Table S7). The footprint analysis revealed that the majority (72–77%) of our measured fluxes originated from the less productive *Nymphaea*-dominated area and only 12–16% originated from the more productive *Typha*-dominated area. Hence, the marsh site showed a relatively weak CO_2 uptake rate in contrast to other reported marshes (e.g., *Typha*-dominated) [Rocha and Goulden, 2008; Rocha and Goulden, 2009]. In addition, Rocha and Goulden [2008] documented that freshwater marshes may have large interannual F_{CO_2} variability even under consistent environmental conditions. In their 5 year study, the annual F_{CO_2} varied drastically from -251 to $515 \text{ g C-CO}_2 \text{ m}^{-2} \text{ yr}^{-1}$. Our study was conducted in two of the warmest years in the last 118 year time span in the region, of which the year 2011 also had an extremely high amount of annual precipitation. Without the baseline F_{CO_2} and F_{CH_4} data of the marsh site, caution is needed in drawing the conclusion that our 2 year research represents a general pattern in freshwater marshes. Long-term research is needed in order to better understand the interannual variability of F_{CH_4} and F_{CO_2} and quantify to what extent the climate extremes may affect the atmospheric carbon budget of freshwater marshes.

Despite the interannual variation, the imbalanced atmospheric carbon budget (especially in 2012) suggests that there is a significant amount of carbon that is unaccounted by our current research framework. Our earlier research indicated that the sediment carbon accumulation rate was around $170 \text{ g C m}^{-2} \text{ yr}^{-1}$ at the same marsh site [Gottgens and Liptak, 1998]. They estimated that roughly 59% ($101 \text{ g C m}^{-2} \text{ yr}^{-1}$) of the deposited carbon originated within the marsh while the rest ($69 \text{ g C m}^{-2} \text{ yr}^{-1}$) was imported from the agricultural

ditches. It should be mentioned that the sedimentation rate they reported was estimated based on ^{210}Pb and ^{137}Cs radioactive dating with a coarse temporal resolution (~ 10 years). However, the long-term carbon accumulation trend suggests that the marsh site is generally a carbon sink and, most importantly, accumulated a considerable amount of carbon from both the primary production within the marsh (autochthonous carbon) and from the lateral hydrological import (allochthonous carbon). Future research is needed, especially to quantify the lateral hydrological carbon transport and sediment carbon deposition rate, in order to improve our estimate of the marsh carbon budget.

The atmospheric carbon budget at the cropland site showed that F_{CH_4} was generally negligible from the soybean cropland. Similar conclusions were drawn by several studies noting that croplands were generally not major sources or sinks of CH_4 [Ruan and Robertson, 2013; Ussiri et al., 2009; Wang et al., 2011; Zenone et al., 2011, 2013]. The reported annual F_{CH_4} ranged from -0.03 to $0.28 \text{ g C-CH}_4 \text{ m}^{-2} \text{ yr}^{-1}$. Ussiri et al. [2009] found that croplands can turn from a minor CH_4 source to a minor sink where tillage practice changes from moldboard plow or chisel tillage to no tillage. Our study showed that F_{CH_4} increased slightly after the harvest and tillage. Additionally, the subsurface soil was frequently saturated and groundwater level was high in the fall and winter of 2011. These factors might lead to slightly higher F_{CH_4} in those periods. However, considering the uncertainties of the flux measurements and the detection limit of the LI7700 at such a low level of F_{CH_4} , the results should be interpreted cautiously.

Based on relative spatial coverage of marshes ($\sim 4\%$), croplands ($\sim 70\%$), and forests ($\sim 7\%$) in the region, the amount of carbon released via CO_2/CH_4 from the marshes should be compensated by the net CO_2 uptake of croplands and forests in the region. On average, the marsh released $\sim 28.7 \text{ g C m}^{-2} \text{ yr}^{-1}$ to the atmosphere in the 2 year study period. On the other hand, our soybean cropland sequestered $\sim 150 \text{ g C-CO}_2 \text{ m}^{-2} \text{ yr}^{-1}$. Xie et al. [2014] reported that an oak-dominated forest in the same region had a 7 year average F_{CO_2} of $-339 \text{ g C-CO}_2 \text{ m}^{-2} \text{ yr}^{-1}$. Zenone et al. [2013] reported that a conventional corn cropland in southwestern Michigan, USA, sequestered $\sim 60 \text{ g C-CO}_2 \text{ m}^{-2} \text{ yr}^{-1}$ via CO_2 uptake in their 3 year study. As marshes occupy only a small portion of area in the region, the atmospheric carbon loss from the wetlands should be compensated by the net CO_2 uptake at croplands and forests in the region. It should be noted that, while CH_4 accounted for a considerable portion of the atmospheric carbon loss from the wetlands, the interplay of CO_2 uptake and CH_4 emission from adjacent ecosystems needs further research in order to better understand the regional greenhouse gas budget and global warming effects.

The importance of hydrologic carbon fluxes among ecosystems is increasingly addressed in recent carbon cycling studies [e.g., Algesten et al., 2004; Cole et al., 2007]. The terrestrial-aquatic continuum concept reveals the significance of hydrologic processes in transporting carbon among ecosystems [Aufdenkampe et al., 2011; Cole et al., 2007; Jenerette and Lal, 2005; Johnson et al., 2008; Richey et al., 2002; Tranvik et al., 2009]. Carbon sequestered by terrestrial ecosystems (e.g., croplands) may be leached and transported via hydrologic processes (e.g., runoff) to adjacent aquatic ecosystems [Buffam et al., 2011]. Consequently, lateral hydrologic carbon processes may be an important vector in relocating carbon among different ecosystems in the landscape. Our marsh site continuously receives inflows from the nearby croplands and the outflow gate is closed most of the time. The organic matter carried by the inflows is likely to be trapped in the marsh and deposited into the sediment and/or released to the atmosphere [Algesten et al., 2004; Buffam et al., 2011; Cole et al., 2007; Kling et al., 1991; Tranvik et al., 2009]. Hence, the carbon uptake at the nearby croplands may contribute to the carbon loss (CO_2 or CH_4) and lead to an imbalanced atmospheric carbon budget in the marsh.

5. Conclusions

Freshwater marshes deserve more research and management attention with respect to their greenhouse effects. Freshwater marshes characterized by deep water and long-lasting inundated conditions are usually dominated by aquatic macrophytes with pressurized ventilation characteristics. The plant-modulated gas flow along with the frequent inundation leads to great CH_4 production/emission potential at these freshwater marshes. In addition, the imbalanced atmospheric carbon budget from our 2 year study suggests that other uncounted carbon (e.g., lateral hydrologic imports, sediment storage) may play a crucial role in marsh carbon cycling. While freshwater marshes account for a small portion of current land use in

agriculture-dominated northwestern Ohio, they are usually located at lower elevations and receive a considerable amount of runoff (and thus nutrients and carbon) from adjacent croplands. Thus, these remaining marshes may act as hot spots in the regional carbon cycling by accumulating carbon in the sediment and/or converting the carbon into CH₄ and releasing it to the atmosphere. Although freshwater marshes are generally not major soil carbon pools in comparison to peat-rich wetlands, their inundated conditions, plant-facilitated gas flow, and hydrologic connections have important implications for their efficiency in turning the newly fixed carbon (either allochthonous or autochthonous) into CH₄ and releasing it to the atmosphere.

Acknowledgments

The F_{CH₄}, F_{CO₂}, and auxiliary micrometeorological data will be archived and available for downloading at the Landscape Ecology and Ecosystem Science (LEES) Lab website (<http://research.eeescience.utoledo.edu/lees/>). This project was funded by the National Oceanic and Atmospheric Administration (NOAA) (NA10OAR4170224) and the National Science Foundation (NSF1034791), USA. We thank John Simpson and the Winous Point Marsh Conservancy for supporting the research platform and logistical assistance at the Winous Point North Marsh. We thank Walter B. Berger for providing his cropland and helping with the infrastructure construction. We thank Ankur R. Desai, Ge Sun, Timothy Fisher, James Martin-Hayden, Donald R. Cahoon, Karen Roderick-Lingema, Scott A. Heckathorn, and Thomas B. Bridgeman for their helpful assistances and advice. Dennis D. Baldocchi, one anonymous Associate Editor, and two anonymous reviewers provided valuable suggestions for the quality of the study. We gratefully acknowledge Mike Deal, Jianye Xu, Orrin Babcock, Cory Becher, Changliang Shao, Yahn-Jauh Su, Jing Xie, Jennifer Teeple, Terenzio Zenone, and Wei Shen for building and maintaining the site infrastructure and assisting in the data collection and management. We also thank Lisa Delp Taylor for editing the manuscript.

References

- Algesten, G., S. Sobek, A.-K. Bergström, A. Ågren, L. J. Tranvik, and M. Jansson (2004), Role of lakes for organic carbon cycling in the boreal zone, *Global Change Biol.*, *10*(1), 141–147, doi:10.1111/j.1365-2486.2003.00721.x.
- Aubinet, M., et al. (2000), Estimates of the annual net carbon and water exchange of forests: The EUROFLUX methodology, *Adv. Ecol. Res.*, *30*, 113–175.
- Aufdenkampe, A. K., E. Mayorga, P. A. Raymond, J. M. Melack, S. C. Doney, S. R. Alin, R. E. Aalto, and K. Yoo (2011), Riverine coupling of biogeochemical cycles between land, oceans, and atmosphere, *Front. Ecol. Environ.*, *9*(1), 53–60, doi:10.1890/100014.
- Baldocchi, D. D., et al. (2001), FLUXNET: A new tool to study the temporal and spatial variability of ecosystem-scale carbon dioxide, water vapor, and energy flux densities, *Bull. Am. Meteorol. Soc.*, *82*(11), 2415–2434.
- Baldocchi, D. D., B. B. Hicks, and T. P. Meyers (1988), Measuring biosphere-atmosphere exchanges of biologically related gases with micrometeorological methods, *Ecology*, *69*(5), 1331–1340.
- Barr, A., T. A. Black, and H. McCanughey (2009), Climate and phenological controls of the carbon and energy balances of three contrasting boreal forest ecosystems in western Canada, in *Phenology of Ecosystem Processes*, edited by A. Noormets, pp. 3–34, Springer, New York.
- Bellio, R., and A. R. Brazzale (2003), Higher order asymptotics unleashed: Software design for nonlinear heteroscedastic regression, *J. Comput. Graph. Stat.*, *12*(3), 682–697, doi:10.1198/1061860032003.
- Bendix, M., T. Tornbjerg, and H. Brix (1994), Internal gas transport in *Typha latifolia* L. and *Typha angustifolia* L. 1. Humidity-induced pressurization and convective throughflow, *Aquat. Bot.*, *49*(2), 75–89.
- Bonan, G. B. (2002), *Ecological Climatology: Concepts and Applications*, 2nd ed., Cambridge Univ. Press, Cambridge, U. K.
- Bousquet, P., et al. (2006), Contribution of anthropogenic and natural sources to atmospheric methane variability, *Nature*, *443*(7110), 439–443.
- Bridgman, S., J. Megonigal, J. Keller, N. Bliss, and C. Trettin (2006), The carbon balance of North American wetlands, *Wetlands*, *26*(4), 889–916, doi:10.1672/0277-5212(2006)26[889:tcbona]2.0.co;2.
- Bridgman, S. D., H. Cadillo-Quiroz, J. K. Keller, and Q. Zhuang (2012), Methane emissions from wetlands: Biogeochemical, microbial, and modeling perspectives from local to global scales, *Global Change Biol.*, *19*(5), 1325–1346, doi:10.1111/gcb.12131.
- Brix, H., B. K. Sorrel, and P. T. Orr (1992), Internal pressurization and convective gas flow in some emergent freshwater macrophytes, *Limnol. Oceanogr.*, *37*(7), 1420–1433.
- Buffam, I., M. G. Turner, A. R. Desai, P. C. Hanson, J. A. Rusak, N. R. Lottig, E. H. Stanley, and S. R. Carpenter (2011), Integrating aquatic and terrestrial components to construct a complete carbon budget for a north temperate lake district, *Global Change Biol.*, *17*(2), 1193–1211, doi:10.1111/j.1365-2486.2010.02313.x.
- Chanton, J., P. Glaser, L. Chasar, D. Burdige, M. Hines, D. Siegel, L. Tremblay, and W. Cooper (2008), Radiocarbon evidence for the importance of surface vegetation on fermentation and methanogenesis in contrasting types of boreal peatlands, *Global Biogeochem. Cycles*, *22*, GB4022, doi:10.1029/2008GB003274.
- Chu, H.-S., et al. (2014), Does canopy wetness matter? Evapotranspiration from a subtropical montane cloud forest in Taiwan, *Hydrol. Processes*, *28*, 1190–1214, doi:10.1002/hyp.9662.
- Chu, H.-S., N.-S. Liang, C.-W. Lai, C.-C. Wu, S.-C. Chang, and Y.-J. Hsia (2013), Topographic effects on CO₂ flux measurement at the Chi-Lan mountain forest site, *Taiwan J. For. Sci.*, *28*(1), 1–16.
- Cole, J., et al. (2007), Plumbing the global carbon cycle: Integrating inland waters into the terrestrial carbon budget, *Ecosystems*, *10*(1), 172–185, doi:10.1007/s10021-006-9013-8.
- Dabberdt, W. F., D. H. Lenschow, T. W. Horst, P. R. Zimmerman, S. P. Oncley, and A. C. Delany (1993), Atmosphere-surface exchange measurements, *Science*, *260*(5113), 1472–1481.
- Dacey, J. (1981), Pressurized ventilation in the yellow waterlily, *Ecology*, *62*(5), 1137–1147, doi:10.2307/1937277.
- Dacey, J., and M. Klug (1979), Methane efflux from lake sediments through water lilies, *Science*, *203*(4386), 1253–1255.
- Dengel, S., P. E. Levy, J. Grace, S. K. Jones, and U. M. Skiba (2011), Methane emissions from sheep pasture, measured with an open-path eddy covariance system, *Global Change Biol.*, *17*(12), 3524–3533, doi:10.1111/j.1365-2486.2011.02466.x.
- Dorodnikov, M., K. Knorr, Y. Kuzyakov, and M. Wilmking (2011), Plant-mediated CH₄ transport and contribution of photosynthates to methanogenesis at a boreal mire: A ¹⁴C pulse-labeling study, *Biogeosciences*, *8*(8), 2365–2375.
- Edwards, G. C., H. H. Neumann, G. den Hartog, G. W. Thurtell, and G. Kidd (1994), Eddy correlation measurements of methane fluxes using a tunable diode laser at the Kinosheo Lake tower site during the Northern Wetlands Study (NOWES), *J. Geophys. Res.*, *99*(D1), 1511–1517, doi:10.1029/93JD02368.
- Forster, P., et al. (2007), Changes in atmospheric constituents and in radiative forcing, in *Climate Change 2007: The Physical Science Basis. Contribution of Working Group I to the Fourth Assessment Report of the Intergovernmental Panel on Climate Change*, edited by S. Solomon et al., pp. 129–234, Cambridge Univ. Press, Cambridge, U. K.
- Frolking, S., N. Roulet, and J. Fuglestedt (2006), How northern peatlands influence the Earth's radiative budget: Sustained methane emission versus sustained carbon sequestration, *J. Geophys. Res.*, *111*, G01008, doi:10.1029/2005JG000091.
- Gottgens, J. F., and M. A. Liptak (1998), Long-term assimilation of agricultural runoff in a Lake Erie marsh, *Verh. Internat. Verein. Limnol.*, *26*, 1337–1342.
- Gottgens, J. F., B. P. Swartz, R. W. Kroll, and M. Eboch (1998), Long-term GIS-based records of habitat changes in a Lake Erie coastal marsh, *Wetlands Ecol. Manage.*, *6*(1), 5–17.

- Grosse, W. (1996), Pressurised ventilation in floating-leaved aquatic macrophytes, *Aquat. Bot.*, *54*(2-3), 137–150.
- Grosse, W., H. Bernhard Büchel, and H. Tiebel (1991), Pressurised ventilation in wetland plants, *Aquat. Bot.*, *39*(1), 89–98.
- Grosse, W., K. Jovy, and H. Tiebel (1996), Influence of plants on redox potential and methane production in water-saturated soil, *Hydrobiologia*, *340*(1-3), 93–99, doi:10.1007/BF00012739.
- Hanis, K. L., M. Tenuta, B. D. Amiro, and T. N. Papakyriakou (2013), Seasonal dynamics of methane emissions from a subarctic fen in the Hudson Bay Lowlands, *Biogeosciences*, *10*, 4465–4479, doi:10.5194/bg-10-4465-2013.
- Hargreaves, K. J., and D. Fowler (1998), Quantifying the effects of water table and soil temperature on the emission of methane from peat wetland at the field scale, *Atmos. Environ.*, *32*(19), 3275–3282, doi:10.1016/s1352-2310(98)00082-x.
- Hatala, J. A., M. Detto, O. Sonnentag, S. J. Deverel, J. Verfaillie, and D. D. Baldocchi (2012), Greenhouse gas (CO₂, CH₄, H₂O) fluxes from drained and flooded agricultural peatlands in the Sacramento-San Joaquin Delta, *Agric. Ecosyst. Environ.*, *150*, 1–18.
- Hendriks, D., J. Van Huissteden, A. Dolman, and M. Van der Molen (2007), The full greenhouse gas balance of an abandoned peat meadow, *Biogeosciences*, *4*, 411–424, doi:10.5194/bg-4-411-2007.
- Herbst, M., T. Friborg, R. Ringgaard, and H. Soegaard (2011a), Catchment-wide atmospheric greenhouse gas exchange as influenced by land use diversity, *Vadose Zone J.*, *10*(1), 67–77.
- Herbst, M., T. Friborg, R. Ringgaard, and H. Soegaard (2011b), Interpreting the variations in atmospheric methane fluxes observed above a restored wetland, *Agric. For. Meteorol.*, *151*(7), 841–853.
- Herbst, M., T. Friborg, K. Schelde, R. Jensen, R. Ringgaard, V. Vasquez, A. G. Thomsen, and H. Soegaard (2013), Climate and site management as driving factors for the atmospheric greenhouse gas exchange of a restored wetland, *Biogeosciences*, *10*, 39–52, doi:10.5194/bg-10-39-2013.
- Jackowicz-Korczyński, M., T. R. Christensen, K. Bäckstrand, P. Crill, T. Friborg, M. Mastepanov, and L. Ström (2010), Annual cycle of methane emission from a subarctic peatland, *J. Geophys. Res.*, *115*, G02009, doi:10.1029/2008JG000913.
- Jenerette, G. D., and R. Lal (2005), Hydrologic sources of carbon cycling uncertainty throughout the terrestrial-aquatic continuum, *Global Change Biol.*, *11*(11), 1873–1882, doi:10.1111/j.1365-2486.2005.01021.x.
- Jialin, L. (2011), Study on the seasonal dynamics of zonal vegetation of NDVI/EVI of costal zonal vegetation based on MODIS data: A case study of *Spartina alterniflora* salt marsh on Jiangsu Coast, China, *Afr. J. Agric. Res.*, *6*(17), 4019.
- Johnson, M. S., J. Lehmann, S. J. Riha, A. V. Krusche, J. E. Richey, J. P. H. B. Ometto, and E. G. Couto (2008), CO₂ efflux from Amazonian headwater streams represents a significant fate for deep soil respiration, *Geophys. Res. Lett.*, *35*, L17401, doi:10.1029/2008GL034619.
- Jung, M., M. Reichstein, P. Ciais, S. I. Seneviratne, J. Sheffield, M. L. Goulden, G. Bonan, A. Cescatti, J. Chen, and R. de Jeu (2010), Recent decline in the global land evapotranspiration trend due to limited moisture supply, *Nature*, *467*(7318), 951–954.
- Kim, J., S. B. Verma, and D. P. Billesbach (1999), Seasonal variation in methane emission from a temperate *Phragmites*-dominated marsh: Effect of growth stage and plant-mediated transport, *Global Change Biol.*, *5*(4), 433–440.
- King, J. Y., W. S. Reeber, K. K. Thieler, G. W. Kling, W. M. Loya, L. C. Johnson, and K. J. Nadelhoffer (2002), Pulse-labeling studies of carbon cycling in Arctic tundra ecosystems: The contribution of photosynthates to methane emission, *Global Biogeochem. Cycles*, *16*(4), 1062, doi:10.1029/2001GB001456.
- Kling, G. W., G. W. Kippbut, and M. C. Miller (1991), Arctic lakes and streams as gas conduits to the atmosphere: Implications for tundra carbon budgets, *Science*, *251*(4991), 298–301, doi:10.1126/science.251.4991.298.
- Kormann, R., and F. Meixner (2001), An analytical footprint model for non-neutral stratification, *Boundary Layer Meteorol.*, *99*(2), 207–224, doi:10.1023/a:1018991015119.
- Kroon, P. S., A. P. Schrier-Uijl, A. Hensen, E. M. Veenendaal, and H. J. J. Jonker (2010), Annual balances of CH₄ and N₂O from a managed fen meadow using eddy covariance flux measurements, *Eur. J. Soil Sci.*, *61*(5), 773–784, doi:10.1111/j.1365-2389.2010.01273.x.
- Le Mer, J., and P. Roger (2001), Production, oxidation, emission and consumption of methane by soils: A review, *Eur. J. Soil Biol.*, *37*(1), 25–50.
- LI-COR (2010), *LI-7700 Open Path CH₄ Analyzer Instruction Manual*, LI-COR, Inc. Biosciences, Lincoln, Nebr.
- Lieth, H. (Ed.) (1974), *Phenology and Seasonality Modeling*, 444 pp., Springer, New York.
- Lundin, E. J., R. Giesler, A. Persson, M. S. Thompson, and J. Karlsson (2013), Integrating carbon emissions from lakes and streams in a subarctic catchment, *J. Geophys. Res. Biogeosci.*, *118*, 1200–1207, doi:10.1002/jgrg.20092.
- Lunetta, R. S., Y. Shao, J. Ediriwickrema, and J. G. Lyon (2010), Monitoring agricultural cropping patterns across the Laurentian Great Lakes Basin using MODIS-NDVI data, *Int. J. Appl. Earth Obs.*, *12*(2), 81–88, doi:10.1016/j.jag.2009.11.005.
- McDermitt, D., et al. (2011), A new low-power, open-path instrument for measuring methane flux by eddy covariance, *Appl. Phys. B-Lasers O.*, *102*(2), 391–405, doi:10.1007/s00340-010-4307-0.
- Mitsch, W., and J. Gosselink (2007), *Wetlands*, 4th ed., Wiley, Hoboken, N. J.
- Mitsch, W. J., B. Bernal, A. M. Nahlik, Ü. Mander, L. Zhang, C. J. Anderson, S. E. Jørgensen, and H. Brix (2012), Wetlands, carbon, and climate change, *Landscape Ecol.*, *28*(4), 583–597.
- Morisette, J. T., et al. (2008), Tracking the rhythm of the seasons in the face of global change: Phenological research in the 21st century, *Front. Ecol. Environ.*, *7*(5), 253–260, doi:10.1890/070217.
- Noormets, A., S. G. McNulty, J. L. DeForest, G. Sun, Q. Li, and J. Chen (2008), Drought during canopy development has lasting effect on annual carbon balance in a deciduous temperate forest, *New Phytol.*, *179*(3), 818–828.
- Olson, D. M., T. J. Griffis, A. Noormets, R. Kolka, and J. Chen (2013), Interannual, seasonal, and retrospective analysis of the methane and carbon dioxide budgets of a temperate peatland, *J. Geophys. Res. Biogeosci.*, *118*, 226–238, doi:10.1002/jgrg.20031.
- Reichstein, M., et al. (2005), On the separation of net ecosystem exchange into assimilation and ecosystem respiration: Review and improved algorithm, *Global Change Biol.*, *11*(9), 1424–1439.
- Richards, J. H., D. N. Kuhn, and K. Bishop (2012), Interrelationships of petiolar air canal architecture, water depth, and convective air flow in *Nymphaea odorata* (Nymphaeaceae), *Am. J. Bot.*, *99*(12), 1903–1909, doi:10.3732/ajb.1200269.
- Richardson, A. D., and D. Y. Hollinger (2005), Statistical modeling of ecosystem respiration using eddy covariance data: Maximum likelihood parameter estimation, and Monte Carlo simulation of model and parameter uncertainty, applied to three simple models, *Agric. For. Meteorol.*, *131*(3–4), 191–208, doi:10.1016/j.agrformet.2005.05.008.
- Richardson, A. D., D. Y. Hollinger, J. D. Aber, S. V. Ollinger, and B. H. Braswell (2007), Environmental variation is directly responsible for short- but not long-term variation in forest-atmosphere carbon exchange, *Global Change Biol.*, *13*(4), 788–803, doi:10.1111/j.1365-2486.2007.01330.x.
- Richey, J. E., J. M. Melack, A. K. Aufdenkampe, V. M. Ballester, and L. L. Hess (2002), Outgassing from Amazonian rivers and wetlands as a large tropical source of atmospheric CO₂, *Nature*, *416*(6881), 617–620.
- Rinne, J., T. Riutta, M. Pihlatie, M. Aurela, S. Haapanala, J. P. Tuovinen, E. S. Tuittila, and T. Vesala (2007), Annual cycle of methane emission from a boreal fen measured by the eddy covariance technique, *Tellus, Ser. B*, *59*(3), 449–457.

- Rocha, A. V., and M. L. Goulden (2008), Large interannual CO₂ and energy exchange variability in a freshwater marsh under consistent environmental conditions, *J. Geophys. Res.*, *113*, G04019, doi:10.1029/2008JG000712.
- Rocha, A. V., and M. L. Goulden (2009), Why is marsh productivity so high? New insights from eddy covariance and biomass measurements in a *Typha* marsh, *Agric. For. Meteorol.*, *149*(1), 159–168, doi:10.1016/j.agrformet.2008.07.010.
- Ruan, L., and G. P. Robertson (2013), Initial nitrous oxide, carbon dioxide and methane costs of converting conservation reserve program grassland to row crops under no-till vs. conventional tillage, *Global Change Biol.*, *19*(8), 2478–2489, doi:10.1111/gcb.12216.
- Schipper, L. A., and K. R. Reddy (1994), Methane production and emissions from four reclaimed and pristine wetlands of southeastern United States, *Soil Sci. Soc. Am. J.*, *58*(4), 1270–1275, doi:10.2136/sssaj1994.03615995005800040039x.
- Sebacher, D. I., R. C. Harriss, and K. B. Bartlett (1985), Methane emissions to the atmosphere through aquatic plants¹, *J. Environ. Qual.*, *14*(1), 40–46, doi:10.2134/jeq1985.00472425001400010008x.
- Song, C., X. Xu, H. Tian, and Y. Wang (2009), Ecosystem–atmosphere exchange of CH₄ and N₂O and ecosystem respiration in wetlands in the Sanjiang Plain, Northeastern China, *Global Change Biol.*, *15*(3), 692–705.
- Ström, L., T. Tagesson, M. Mastepanov, and T. R. Christensen (2012), Presence of *Eriophorum scheuchzeri* enhances substrate availability and methane emission in an Arctic wetland, *Soil Biol. Biochem.*, *45*, 61–70.
- Tagesson, T., M. Mölder, M. Mastepanov, C. Sigsgaard, M. P. Tamstorf, M. Lund, J. M. Falk, A. Lindroth, T. R. Christensen, and L. Ström (2012), Land-atmosphere exchange of methane from soil thawing to soil freezing in a high-Arctic wet tundra ecosystem, *Global Change Biol.*, *18*(6), 1928–1940, doi:10.1111/j.1365-2486.2012.02647.x.
- Tan, Z.-H., et al. (2012), An observational study of the carbon-sink strength of East Asian subtropical evergreen forests, *Environ. Res. Lett.*, *7*(4), 044,017.
- Teklemariam, T. A., P. M. Lafleur, T. R. Moore, N. T. Roulet, and E. R. Humphreys (2010), The direct and indirect effects of inter-annual meteorological variability on ecosystem carbon dioxide exchange at a temperate ombrotrophic bog, *Agric. For. Meteorol.*, *150*(11), 1402–1411.
- Tornberg, T., M. Bendix, and H. Brix (1994), Internal gas transport in *Typha latifolia* L. and *Typha angustifolia* L. 2. Convective throughflow pathways and ecological significance, *Aquat. Bot.*, *49*(2), 91–105.
- Tranvik, L. J., et al. (2009), Lakes and reservoirs as regulators of carbon cycling and climate, *Limnol. Oceanogr.*, *54*(6 (part 2)), 2298–2314, 6985126.
- Ussiri, D. A. N., R. Lal, and M. K. Jarecki (2009), Nitrous oxide and methane emissions from long-term tillage under a continuous corn cropping system in Ohio, *Soil Till. Res.*, *104*(2), 247–255.
- Verma, S., F. Ullman, D. Billesbach, R. Clement, J. Kim, and E. S. Verry (1992), Eddy correlation measurements of methane flux in a northern peatland ecosystem, *Boundary Layer Meteorol.*, *58*(3), 289–304, doi:10.1007/bf02033829.
- Wang, W., R. C. Dalal, S. H. Reeves, K. Butterbach-Bahl, and R. Kiese (2011), Greenhouse gas fluxes from an Australian subtropical cropland under long-term contrasting management regimes, *Global Change Biol.*, *17*(10), 3089–3101, doi:10.1111/j.1365-2486.2011.02458.x.
- Whalen, S. C. (2005), Biogeochemistry of methane exchange between natural wetlands and the atmosphere, *Environ. Eng. Sci.*, *22*(1), 73–94, doi:10.1089/ees.2005.22.73.
- Whiting, G. J., and J. P. Chanton (1996), Control of the diurnal pattern of methane emission from emergent aquatic macrophytes by gas transport mechanisms, *Aquat. Bot.*, *54*(2–3), 237–253.
- Wille, C., L. Kutzbach, T. Sachs, D. Wagner, and E.-M. Pfeiffer (2008), Methane emission from Siberian arctic polygonal tundra: Eddy covariance measurements and modeling, *Global Change Biol.*, *14*(6), 1395–1408, doi:10.1111/j.1365-2486.2008.01586.x.
- Wu, J., L. van der Linden, G. Lasslop, N. Carvalhais, K. Pilegaard, C. Beier, and A. Ibrom (2012), Effects of climate variability and functional changes on the interannual variation of the carbon balance in a temperate deciduous forest, *Biogeosciences*, *9*, 13–28, doi:10.5194/bg-9-13-2012.
- Xiao, X., J. Zhang, H. Yan, W. Wu, and C. Biradar (2009), Land surface phenology, in *Phenology of Ecosystem Processes*, edited by A. Noormets, pp. 247–270, Springer, New York.
- Xie, J., J. Chen, G. Sun, H. Chu, A. Noormets, Z. Ouyang, R. John, S. Wan, and W. Guan (2014), Long-term variability and environmental control of the carbon cycle in an oak-dominated temperate forest, *Forest Ecol. Manage.*, *313*, 319–328.
- Yi, C., et al. (2010), Climate control of terrestrial carbon exchange across biomes and continents, *Environ. Res. Lett.*, *5*(3), 034,007.
- Yu, L., H. Wang, G. Wang, W. Song, Y. Huang, S.-G. Li, N. Liang, Y. Tang, and J.-S. He (2013), A comparison of methane emission measurements using eddy covariance and manual and automated chamber-based techniques in Tibetan Plateau alpine wetland, *Environ. Pollut.*, *181*, 81–90.
- Zenone, T., J. Chen, M. W. Deal, B. Wilske, P. Jasrotia, J. Xu, A. K. Bhardwaj, S. K. Hamilton, and G. P. Robertson (2011), CO₂ fluxes of transitional bioenergy crops: Effect of land conversion during the first year of cultivation, *Global Change Biol. Bioenergy*, *3*(5), 401–412, doi:10.1111/j.1757-1707.2011.01098.x.
- Zenone, T., I. Gelfand, J. Chen, S. K. Hamilton, and G. P. Robertson (2013), From set-aside grassland to annual and perennial cellulosic biofuel crops: Effects of land use change on carbon balance, *Agric. For. Meteorol.*, *182–183*, 1–12.
- Zhang, X., M. A. Friedl, C. B. Schaaf, A. H. Strahler, J. C. Hodges, F. Gao, B. C. Reed, and A. Huete (2003), Monitoring vegetation phenology using MODIS, *Remote Sens. Environ.*, *84*(3), 471–475.